Article

A *Plasmodium falciparum* ATP-binding cassette transporter is essential for liver stage entry into schizogony

Pf ABCC2 is expressed at the PPM of early - to - mid liver stage schizonts

ABCC2 at PPM

WT

Pf abcc2⁻

Pf abcc2⁻ arrests early during liver stage development and does not generate exo-erythrocytic merozoites.

Pf ABCC2 is expressed at the PPM throughout the asexual blood stage

Pf abcc2⁻ displays a modest growth defect under conditions of extreme nutrient stress

Debashree Goswami, Sudhir Kumar, William Betz, ..., Sean C. Murphy, Ashley M. Vaughan, Stefan H.I. Kappe

stefan.kappe@seattlechildrens.org

Highlights

Pf ABCC2 expression marks the transition from sporozoite to early liver stage

Pf ABCC2 localizes to the early and mid-liver stage plasma membrane

Pf ABCC2 is critical for initiation of exoerythro-cytic schizogony

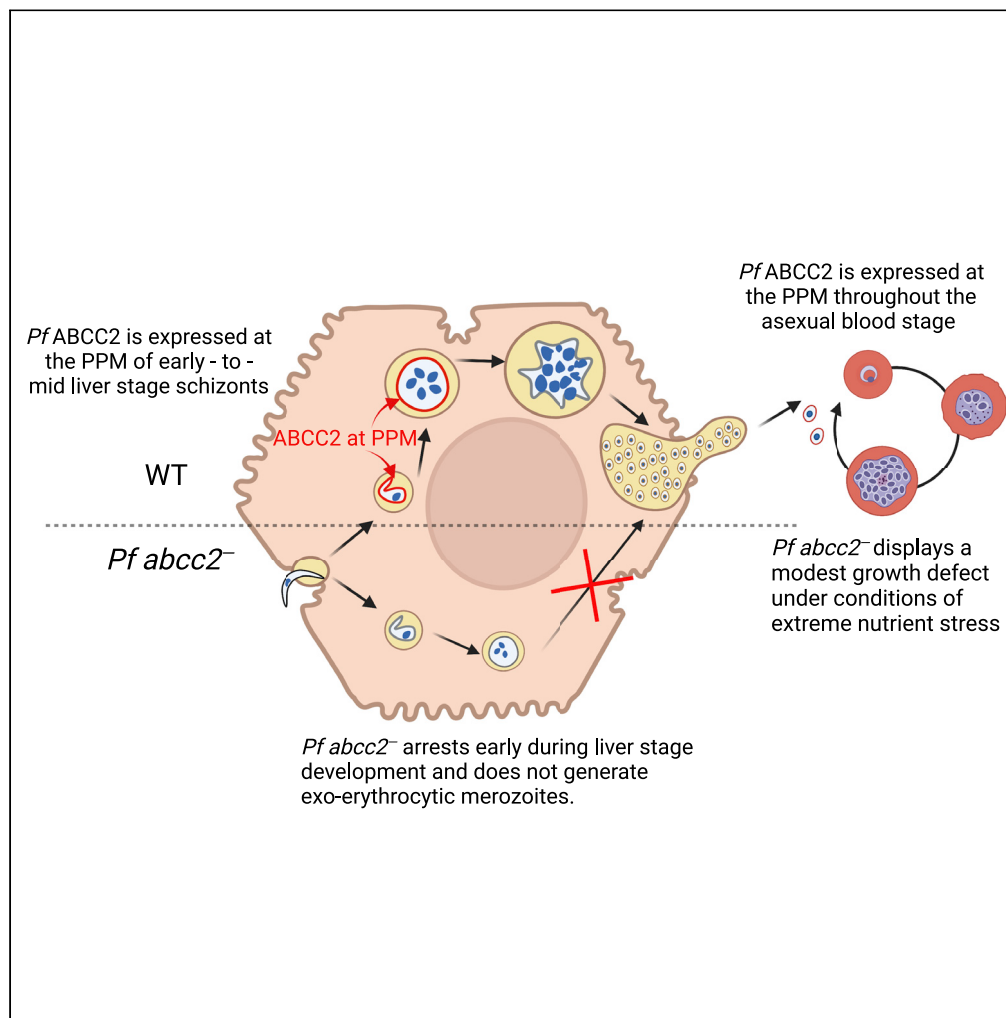*Pf abcc2⁻* liver stages fail to transition to blood stage infection

Article

A *Plasmodium falciparum* ATP-binding cassette transporter is essential for liver stage entry into schizogony

Debashree Goswami,[1] Sudhir Kumar,[1,4] William Betz,[1,4] Janna M. Armstrong,[1] Meseret T. Haile,[1] Nelly Camargo,[1] Chaitra Parthiban,[2] Annette M. Seilie,[2] Sean C. Murphy,[2] Ashley M. Vaughan,[1,3] and Stefan H.I. Kappe[1,3,5,*]

SUMMARY

***Plasmodium* sporozoites invade hepatocytes and transform into liver stages within a parasitophorous vacuole (PV). The parasites then grow and replicate their genome to form exoerythrocytic merozoites that infect red blood cells. We report that the human malaria parasite *Plasmodium falciparum (Pf)* expresses a C-type ATP-binding cassette transporter, *Pf* ABCC2, which marks the transition from invasive sporozoite to intrahepatocytic early liver stage. Using a humanized mouse infection model, we show that *Pf* ABCC2 localizes to the parasite plasma membrane in early and mid-liver stage parasites but is not detectable in late liver stages. *Pf abcc2⁻* sporozoites invade hepatocytes, form a PV, and transform into liver stage trophozoites but cannot transition to exoerythrocytic schizogony and fail to transition to blood stage infection. Thus, *Pf* ABCC2 is an expression marker for early phases of parasite liver infection and plays an essential role in the successful initiation of liver stage replication.**

INTRODUCTION

Malaria caused by *Plasmodium* parasites continues to be a great global health concern. There were 240 million malaria cases with an estimated 627,000 deaths in 2020, which is a significant increase when compared to the previous years (World Health Organization, 2021). Among *Plasmodium* parasites that infect humans, *Plasmodium falciparum (Pf)* causes most morbidity and mortality (World Health Organization, 2021). Transmission of *Pf* to the human host occurs when motile sporozoites are released from the salivary glands and injected into the skin via the bite of an infected female *Anopheles* mosquito (Vaughan and Kappe, 2017; Loubens et al., 2020; Arredondo et al., 2021). Once sporozoites enter the bloodstream, they are transported to the liver and enter the parenchyma to target hepatocytes. Successful infection of hepatocytes requires the formation of a membrane-bound parasitophorous vacuole (PV), in which the invasive sporozoite dedifferentiates and transforms into a liver stage trophozoite (Arredondo et al., 2021). The liver stage trophozoite then undergoes an extensive growth and replication process called exoerythrocytic schizogony that involves cell mass expansion and numerous rounds of genome and organellar replication. A mature late liver stage schizont ultimately differentiates into tens of thousands of exoerythrocytic merozoites, which initiate the symptomatic erythrocytic cycle of infection. A relatively small number of sporozoites are injected into the skin, and an even smaller number of these sporozoites reach the liver via the circulation, rendering the liver stage a critical population bottleneck (Medica and Sinnis, 2005) and an attractive target for prophylactic drug and vaccine development (Kreutzfeld et al., 2017; Vaughan et al., 2017; Draper et al., 2018; Duffy and Gorres, 2020). However, there is an insufficient understanding of *Plasmodium* liver stage biology and most of our knowledge is derived from studies using the rodent malaria models *Plasmodium berghei (Pb)* and *Plasmodium yoelii (Py)*. Thus, *Pf* liver stage development remains largely unexplored because the development of robust liver infection models for human parasites has been challenging.

In the recent years, significant progress has been made in identifying *Pf* proteins required for sporozoite traversal and invasion into hepatocytes (Arredondo et al., 2021). However, there are no known protein markers for early *Pf* liver stage differentiation and development, which should not be expressed in sporozoites but are expressed following sporozoite invasion of hepatocytes. Pioneering studies on sporozoite

[1]Center for Global Infectious Disease Research, Seattle Children's Research Institute, 307 Westlake Avenue N, Seattle, WA, USA

[2]Department of Laboratory Medicine and Pathology and Department of Microbiology, University of Washington, Seattle, WA, USA

[3]Department of Pediatrics, University of Washington, Seattle, WA, USA

[4]These authors contributed equally

[5]Lead contact

*Correspondence:
stefan.kappe@seattlechildrens.org

https://doi.org/10.1016/j.isci.2022.104224

biology in the rodent malaria species *Pb* identified transcripts that are Upregulated in Infective Sporozoites (UIS) by subtractive cDNA hybridization (Kappe et al., 2001). These genes are highly transcribed in salivary gland sporozoites but remain translationally repressed such that the majority of protein expression is initiated during or just after productive hepatocyte invasion (Lindner et al., 2019). Two such UIS proteins in rodent malaria parasite species are UIS3 (Mueller et al., 2005b; Tarun et al., 2007) and UIS4 (Mueller et al., 2005a), which localize to the PV membrane. Gene-deficient parasites of both UIS3 and UIS4 in *Py* and *Pb* undergo partial arrest early in liver stage development (Mueller et al., 2005a, 2005b; Jobe et al., 2007; Tarun et al., 2007). However, the orthologous UIS3 gene in *Pf* has been refractory to gene deletion, and therefore the role of *Pf* UIS3 in liver stage development remains elusive. The *Pf* gene syntenic to *Pb* and *Py* UIS4, known as *Pf* ETRAMP10.3, is expressed in salivary gland sporozoites (MacKellar et al., 2010; Lindner et al., 2019; Marin-mogollon et al., 2019), late liver stages, and gametocytes (MacKellar et al., 2010; Marin-mogollon et al., 2019). *Pf* ETRAMP10.3 is therefore not useful as a marker for early *Pf* liver stage infection. *Pf* ETRAMP10.3 has also been refractory to gene deletion (MacKellar et al., 2010). Additional UIS proteins, including members of the 6-Cys family of proteins, *Pf* P36 and P52 (Ishino et al., 2005; van Dijk et al., 2005; Labaied et al., 2007; Vanbuskirk et al., 2009), are expressed in salivary gland sporozoites but not in early liver stages, and their deletion prevents the parasite from forming a PV. Thus, no unique markers of early *Pf* liver stage development are available yet.

The *Pf* C-type ATP-binding complex (ABC) transporter proteins, *Pf* ABCC1 and *Pf* ABCC2, were reported to be expressed in *Pf* replicating exoerythrocytic schizonts grown in cultured primary human hepatocytes (Rijpma et al., 2016). Gene deletion studies showed that *Pf abcc1⁻* liver stages developed normally in primary hepatocyte cultures, but *Pf abcc2⁻* liver stages suffered a developmental arrest and did not form mature exoerythrocytic schizonts (Rijpma et al., 2016). Thus, we explored whether *Pf* ABCC2 could serve as a marker for early *Pf* liver stage infection. *Pf* ABCC2 belongs to the ABC family of transporters, which constitute a highly conserved protein superfamily, that utilize the energy from ATP hydrolysis to export a wide range of substrates across cell membranes (Hollenstein et al., 2007; Upton et al., 2011; Wilkens, 2015). Proteins belonging to the ABC transporter family C (ABCC) are also commonly referred to as multidrug resistance-associated proteins (MRPs). MRP transporters are known to export organic anions such as glutathione (GSH) conjugates, glucuronide conjugates, and sulfate conjugates across biological membranes (Jones and George, 2007). The genomes of human malaria causing *Plasmodium* species, *Pf*, and *Plasmodium vivax (Pv)* contain two genes belonging to the ABCC subfamily, *ABCC1* and *ABCC2*, whereas the rodent malaria species, *Py* and *Pb*, contain only one ABCC gene (Koenderink et al., 2010).

In this study, we report that *Pf* ABCC2 is not expressed in sporozoites but expression initiates in early liver stages, where the protein localizes to the parasite plasma membrane. Using a humanized mouse model of *Pf* liver stage infection, we show that *Pf* ABCC2 is critical for successful initiation of liver stage parasite growth and replication. Thus, *Pf* ABCC2 can serve as a protein that marks the successful transition to liver stage infection, and it likely plays a role in a critical exchange between the early liver stage cytoplasm and PV lumen.

RESULTS

Pf ABCC2 localizes to the parasite plasma membrane in blood stage parasites and in early- to mid-phases of liver stage development

To evaluate the spatiotemporal localization of *Pf* ABCC2 throughout the parasite life cycle, we generated a transgenic *Pf* NF54 *ABCC2* line using CRISPR/Cas9 gene editing tools (Goswami et al., 2020) that express ABCC2 with a C-terminal mCherry fusion tag (Figure S1A). *Pf ABCC2*^mCherry clones were isolated by limiting dilution cloning. We then investigated blood stage expression of *Pf* ABCC2 via immunofluorescence assay (IFA) using antibodies against mCherry and MSP1 to detect *Pf* ABCC2 and mark the parasite plasma membrane (PPM), respectively. *Pf* ABCC2 expression was detected in intraerythrocytic parasite stages, including trophozoite and schizont stages (Figure 1A). *Pf* ABCC2 was co-localized with MSP1, indicating that it is likely positioned in the PPM. In early schizonts and segmenting schizonts, *Pf* ABCC2 was visible on plasma membrane invaginations (Figure 1A). Interestingly, *Pf* ABCC2 was also observed on the plasma membrane of free merozoites (Figure 1A). No differences in asexual blood stage growth kinetics under standard culture conditions were seen when comparing *Pf* NF54 and *Pf ABCC2*^mCherry strains (Figures S1B). Therefore, fusion of the C-terminal mCherry tag to the *Pf* ABCC2 protein did not affect asexual blood stage development.
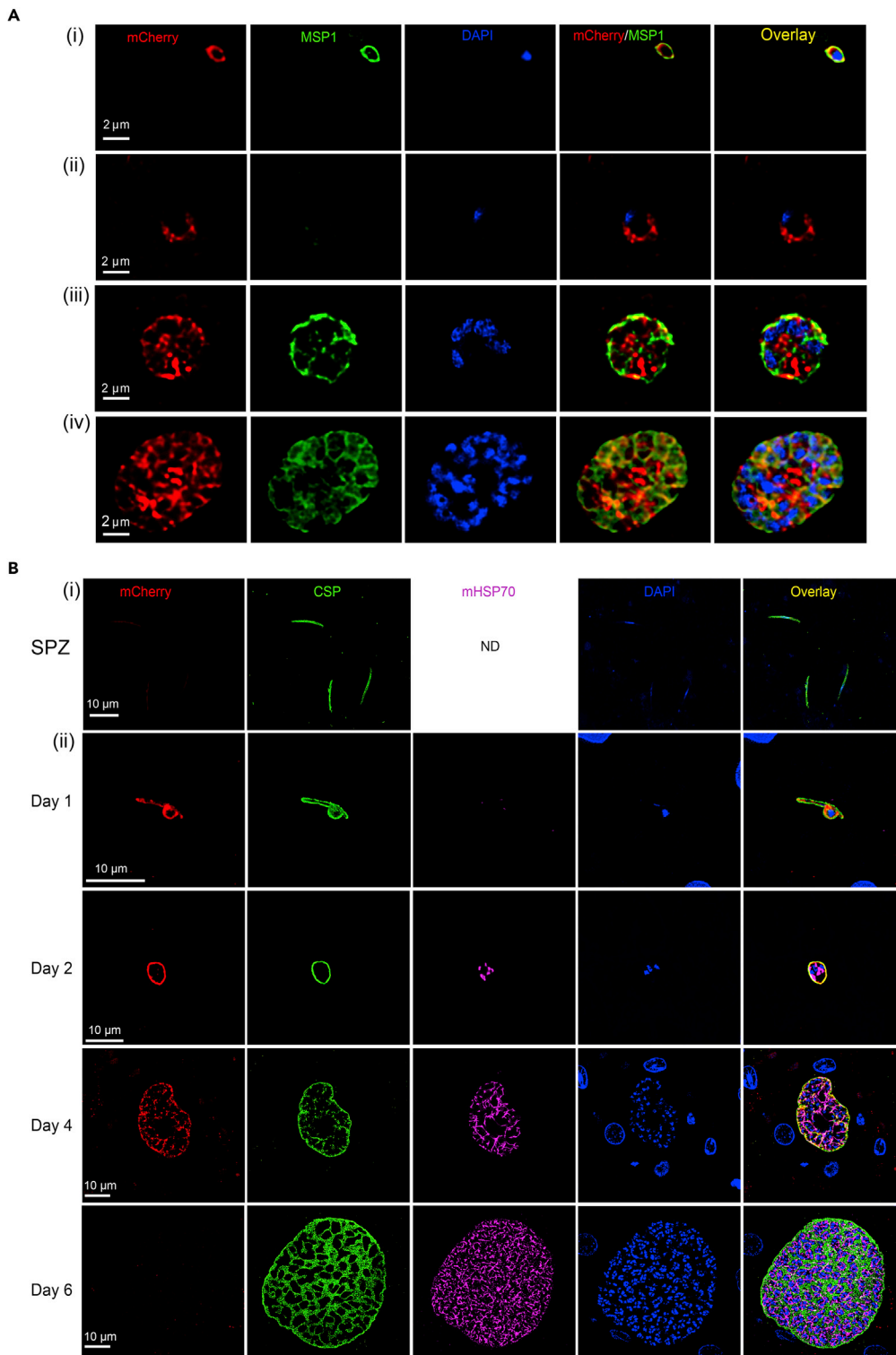
Figure 1. *Pf* ABCC2 localizes to the parasite plasma membrane in *Pf* blood and liver stages

(A) *Pf ABCC2^mCherry* blood stage parasites, (i) merozoite, (ii) ring, (iii) trophozoite, and (iv) schizont, were analyzed by IFA using antibodies against mCherry (red) and MSP1 (green). DNA is stained by DAPI. Scale bar size is 2 μm. *Pf ABCC2^mCherry* localization to the parasite plasma membrane (PPM) was observed in all stages of the intraerythrocytic development and free merozoites as indicated by co-localization with the PPM marker MSP1.

Figure 1. Continued

(B) (i) IFA of *Pf ABCC2^mCherry* salivary gland sporozoites dissected on day 15 of mosquito infection, using antibodies against mCherry (red) and CSP (green). DNA is stained with DAPI. Scale bar size is 10 μm. No *Pf ABCC2^mCherry* expression could be detected in salivary sporozoites. (ii) FRG NOD huHep mice were infected with one million sporozoites of *Pf* ABCC2^mCherry and livers were harvested 1-, 2-, 4-, and 6-days post sporozoite infection. Tissue sections were used for IFAs with antibodies against mCherry to localize ABCC2 (red), the PPM (CSP, green), and the parasite mitochondria (mHSP70, pink). DNA was stained with DAPI. Scale bar size is 10 μm. *Pf ABCC2^mCherry* expression was detected as early as day 1 and persisted until day 4 postinfection. Expression of ABCC2 co-localized with the PPM marker CSP. No *Pf* ABCC2^mCherry expression was detected on day 6.

Pf ABCC2^mCherry parasites also showed normal mosquito stage development as counts for oocysts/midgut, oocyst prevalence, and salivary gland sporozoites/mosquito were within the range of what is observed in wildtype *Pf* NF54 infections (Figure S1C). We analyzed the expression of *Pf* ABCC2 in developing *Pf ABCC2^mCherry* midgut oocysts on day 8 and on mature salivary gland sporozoites on day 15 after an infectious blood meal, both by live microscopy and by IFAs with antibodies against the mCherry tag. No *Pf* ABCC2^mCherry expression was detected in midgut oocysts (Figure S1D) and salivary gland sporozoites (Figures 1B(i), S1E).

We next analyzed the expression dynamics of *Pf* ABCC2 throughout *Pf* liver stage development. Salivary gland sporozoites of the *Pf ABCC2^mCherry* strain were used to infect FRG NOD huHep mice that harbor human hepatocytes (Azuma et al., 2007) as previously described (Goswami et al., 2020), and livers were harvested on 1–6 days after infection. Infected liver tissue sections were analyzed by IFA using antibodies against mCherry, CSP, and mitochondrial HSP70 (mHSP70) to detect expression of *Pf* ABCC2 and visualize the PPM and the parasite mitochondria, respectively. *Pf ABCC2^mCherry* co-localized with CSP to the PPM as early as day 1 of intrahepatocytic parasite development, a time point when sporozoites undergo transformation into trophozoites. Expression continued on day 2 early liver stages and on day 4 liver stage schizonts (Figure 1B(ii)). Interestingly, *Pf* ABCC2 expression appeared to cease in late liver stage schizonts on day 6 after infection (Figure 1B(ii)). No *Pf ABCC2^mCherry* expression was observed within the liver stage cytoplasm or mitochondria. These results indicate that *Pf* ABCC2 is not expressed in sporozoites, but expression is initiated in early liver stage development and continues into mid-liver stage schizogony. However, protein expression does not persist in late liver stage schizonts.

Pf ABCC2 is critical for the initiation of exoerythrocytic schizogony

To investigate the role of *Pf* ABCC2 in liver stage development, we generated *Pf abcc2⁻* gene deletion parasites in the *Pf* NF54 strain via CRISPR/Cas9-mediated gene editing as previously described (Goswami et al., 2020). Successful recombination was confirmed by PCR genotyping and recombinant parasite populations were cloned by limiting dilution (Figure 2A). *Pf abcc2⁻* clones 2F3 and IG7 were used for further phenotypic analysis. *Pf abcc2⁻* gametocytes and wildtype *Pf* NF54 gametocytes were fed to *Anopheles stephensi* mosquitoes in standard membrane feeding assays. Quantitative analysis of mosquito infection showed that the number of oocysts/midgut, oocyst prevalence, and number of salivary gland sporozoites/mosquito were comparable between *Pf abcc2⁻* and *Pf* NF54 parasites (Figure 2B).

To evaluate the role of *Pf* ABCC2 in liver stage development, one million *Pf abcc2⁻* and *Pf* NF54 sporozoites were injected intravenously (i.v.) into FRG huHep mice. Infected livers were harvested on days 2, 3, and 6 postinfection, and liver stage development was compared between *Pf abcc2⁻* and *Pf* NF54 parasites by IFA. Antibodies against CSP, BiP, EXP1, and mHSP70 were used, which mark the PPM, the ER, the PV membrane (PVM), and mitochondria of the parasite, respectively (Figures 3 and S2). *Pf abcc2⁻* sporozoites were able to infect hepatocytes and transform into intrahepatocytic trophozoites as seen on day 2 postinfection (Figure 3A). PVM formation appeared normal in *Pf abcc2⁻* liver stages (Figure S2A). However, *Pf abcc2⁻* parasites were arrested in early liver stage development (Figures 3A(i), (ii)). A large fraction of *Pf abcc2⁻* liver stages were arrested while undergoing the developmental transition from sporozoites into trophozoites (Figure S2B). On day 2 postinfection, approximately 82% *Pf abcc2⁻* liver stages were observed in this stage. This was reduced to 45% on days 3 and 6 with a concomitant increase in the number of fully rounded liver stage trophozoites, indicating that a certain percentage of *Pf abcc2⁻* parasites undergo further differentiation. No difference in the numbers of infected hepatocytes was observed between *Pf abcc2⁻* parasites and *Pf* NF54 (Figure S2C). There was a slight increase in the size of *Pf abcc2⁻* liver stages from day 2 to day 3 (23 μm²–30 μm²), but this difference was not statistically significant (Figure 3A(ii)). There was no additional increase in the size of *Pf abcc2⁻* liver stages from day 3 to day 6. In contrast, *Pf* NF54 liver stage trophozoites
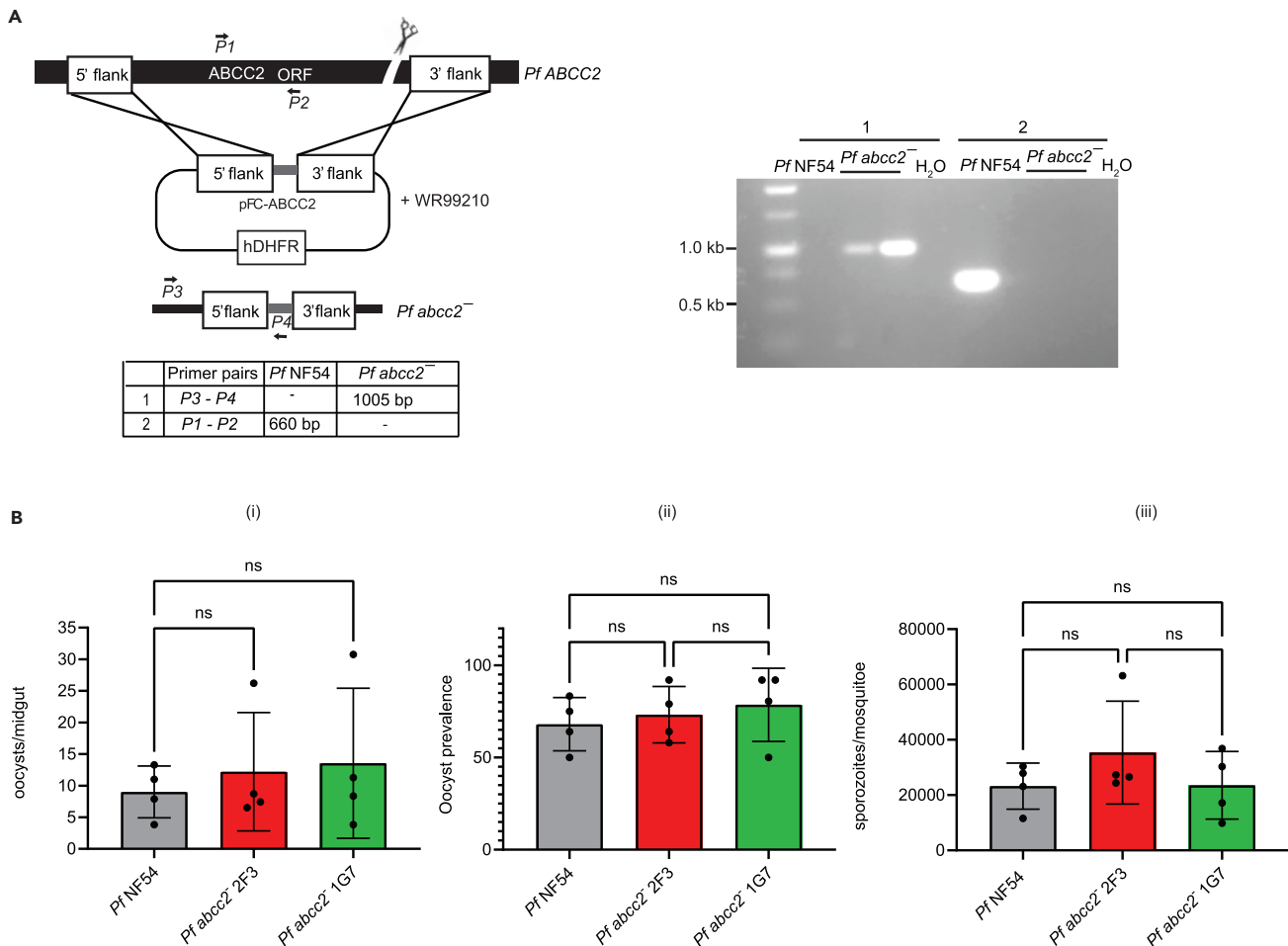
A

B

Figure 2. Pf ABCC2 gene knockout and analysis of mosquito stage development

(A) The schematic depicts the generation of *Pf abcc2⁻* knockout parasites using CRISPR/Cas9-mediated gene editing. Primers used to verify the gene deletion are indicated and the sizes of the PCR amplicons are shown in base pairs. Agarose gel electrophoresis shows the PCR products corresponding to the gene deletion of *Pf abcc2⁻* in clones 2F3 and 1G7.

(B) Mature gametocyte cultures of *Pf* NF54 wild-type parasites (black) and *Pf abcc2⁻* clones 2F3 (red) and 1G7 (green) were fed to female *Anopheles stephensi* mosquitoes in a standard membrane feeding assay. Mosquito midguts were dissected on day 8 for oocyst enumeration and salivary glands were dissected on day 15 post membrane feeding assay for sporozoite enumeration. Graphs comparing (i) the counts for oocyst/midgut (ii) oocyst prevalence (iii) counts for salivary gland sporozoites/mosquito for *Pf* NF54 (black) and *Pf abcc2⁻* clones 2F3 (red) and 1G7 (green). Data are represented as mean $\pm$ SD, n = 4 biological replicates. Statistical analysis was carried out using two-way ANOVA using Tukey's multiple comparison test. "ns" not significant. $p > 0.05$ is taken as not significant.

(day 2) grew and differentiated normally as exoerythrocytic schizonts with a large increase in liver stage size from day 2 to day 6 (70 μm^2–8000 μm^2).

At the time point of growth arrest, numerous *Pf abcc2⁻* liver stages had initiated exoerythrocytic schizogony, indicated by branching of the ER (Figure 3A) and mitochondria (Figure 3B). Although *Pf abcc2⁻* liver stages on day 6 exhibited some segregated DNA centers as visualized by immunostaining with an antibody against the acetylated histone marker, H3K9Ac3 (Figure 3C), genome replication appeared very limited. In contrast, *Pf* NF54 parasites on day 6 had undergone extensive organelle and genome replication (Figures 3A–3C).

Pf abcc2⁻ liver stages fail to transition to blood stage infection

Pf abcc2⁻ liver stages arrest early in the developmental transition of the intrahepatocytic sporozoite to the trophozoite stage and to some degree in early exoerythrocytic schizogony, and lack significant genome
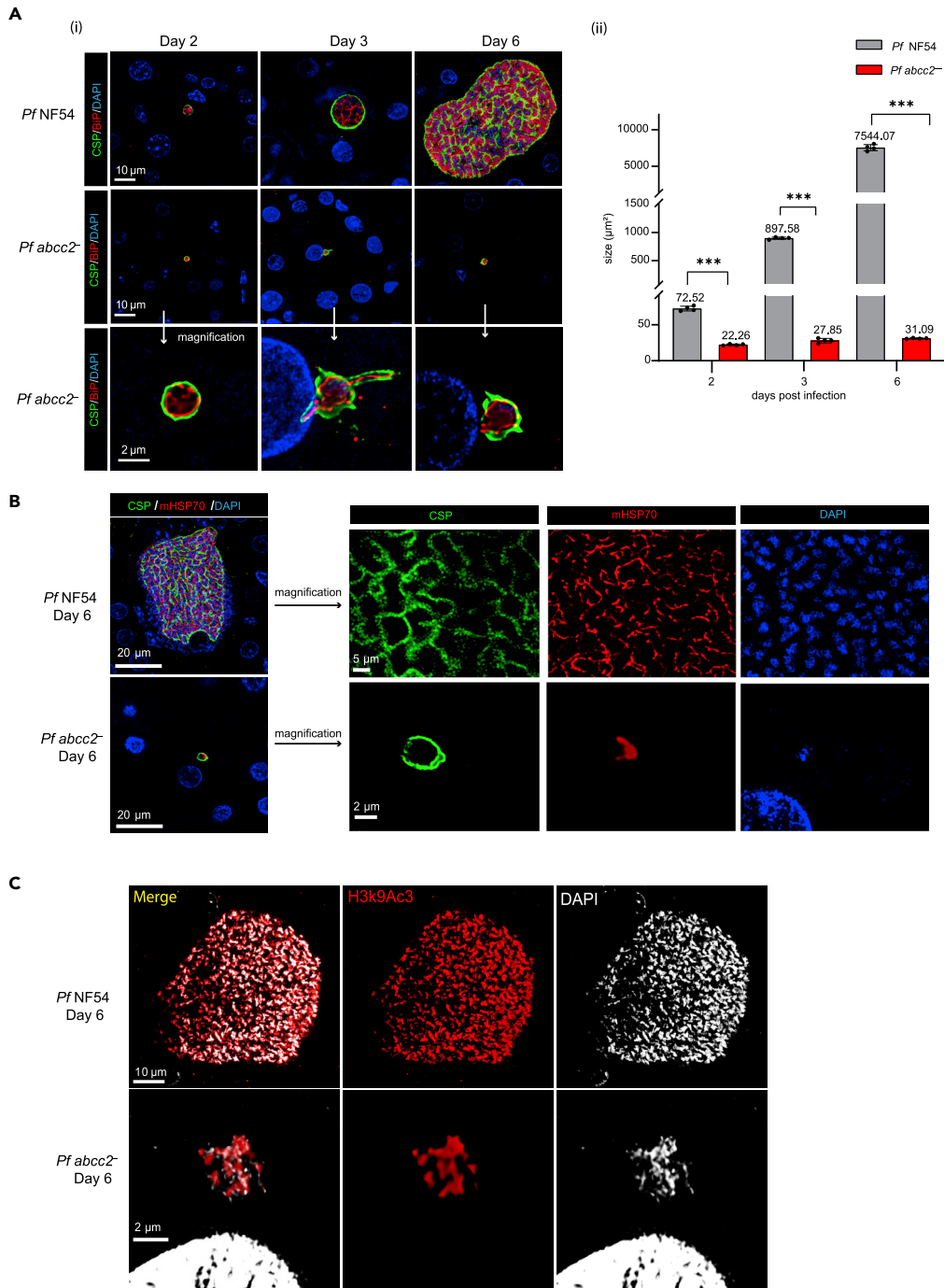
Figure 3. Analysis of *Pf abcc2⁻* liver stage development

Tissue sections were prepared from FRG huHep mice that were infected with one million sporozoites of either *Pf* NF54 or *Pf abcc2⁻* on days 2, 3, and 6 post-sporozoite infection and analyzed by IFA.

(A) (i) Top panels: Liver stage development was compared between *Pf* NF54 and *Pf abcc2⁻* on days 2, 3, and 6 using antibodies against CSP (green) to mark the PPM and the ER marker BiP (red). DNA is stained with DAPI (blue). Scale bar size is 10 μm. *Pf abcc2⁻* parasites arrest very early in liver stage development. Bottom Panel: Magnified images of *Pf abcc2⁻* on days 2, 3, and 6 from the middle panel. Scale bar is 2 μm (ii) Comparison of the size of liver stage parasites (based on area at the parasite's largest circumference) between *Pf* NF54 and *Pf abcc2⁻* on days 2, 3, and 6 post infection. *Pf* NF54 wildtype liver stage schizonts are significantly larger than *Pf abcc2⁻* on days 2, 3, and 6, with a massive difference apparent on day 6. Data are represented as mean ± SD. Each datapoint refers to the mean size of at least 20 parasites per lobe and

Figure 3. Continued

four lobes were analyzed per mouse for each time point. Statistical analysis was carried out using two-way ANOVA using Tukey's multiple comparison test. ***p < 0.001, p > 0.05 is taken as ns.

(B) IFA comparing the cell growth and organellar development between *Pf* NF54 and *Pf abcc2⁻* on day 6 post sporozoite infection using antibodies against the PPM (CSP, green) and parasite mitochondria (mHSP70, red). DNA is stained with DAPI (blue). Scale bar size is 20 μm. The right panels represent a higher magnification image. Scale bar is 5 μm for *Pf* NF54 and 2 μm for *Pf abcc2⁻* .

(C) IFA comparing genome replication between *Pf* NF54 or *Pf abcc2⁻* on day 6 post sporozoite infection using antibodies against acetylated histone (H3K9Ac3, red). DNA is stained with DAPI (white). Scale bar size is 10 μm for *Pf* NF54 and 2 μm for *Pf abcc2⁻*.

and organelle replication (Figure 3). To elucidate whether *Pf abcc2⁻* liver stages express any markers for late liver stage differentiation and exoerythrocytic merozoite formation, IFAs were performed on liver sections of *Pf* NF54 and *Pf abcc2⁻*-infected mice at day 6 postinfection, using antibodies against CSP; this marks the PPM, and MSP1, which labels the PPM and additionally acts as a marker for exoerythrocytic merozoite formation (Goswami et al., 2020). Day 6 *Pf abcc2⁻* liver stages did not express MSP1 (Figure 4A). However, histological analysis of liver stage infection is not sufficiently sensitive to detect rare liver stage forms that could complete exoerythrocytic schizogony, form exoerythrocytic merozoites, and transition to blood stage infection. We have previously shown that the FRG huHep liver-chimeric mouse model constitutes a powerful *in vivo* model to assess *Pf* liver stage exoerythrocytic merozoite transition to blood stage infection (liver-to-blood stage transition) (Vaughan et al., 2012; Foquet et al., 2018; Goswami et al., 2020). Thus, to evaluate whether *Pf abcc2⁻* liver stage growth arrest completely abrogates the formation of any infectious exoerythrocytic merozoites, we conducted liver-to-blood stage transition experiments in FRG huHep mice. We injected 100,000 *Pf* NF54 sporozoites or 100,000 *Pf abcc2⁻* sporozoites i.v. into two FRG huHep mice each; in addition, we dose escalated to one million sporozoites of *Pf abcc2⁻* into five additional FRG NOD huHep mice each (Figure 4B). To detect the transition of exoerythrocytic merozoites into the blood, human red blood cells (RBCs) were injected on days 6 and 7 post-sporozoite infection as described previously (Vaughan et al., 2012; Foquet et al., 2018). On day 7, all mice that had been administered 100,000 sporozoites (either *Pf* NF54 or *Pf abcc2⁻*) were euthanized and exsanguinated. We next employed a highly sensitive *Pf* 18S rRNA qRT-PCR assay that has been used as a diagnostic tool in controlled human malaria infection (CHMI) studies (Seilie et al., 2019). This assay can detect a single ring stage parasite in 50 μL of whole blood (20 parasite equivalents/1 mL of blood), which corresponds to 7400 *Pf* 18S rRNA copies/mL of blood (Walther et al., 2005; Hodgson et al., 2015). Fifty μL of whole blood from infected FRG huHep mice was analyzed by qRT PCR and remaining blood was transferred to *in vitro* blood stage culture with human RBCs. Blood samples of both mice infected with 100,000 *Pf* NF54 sporozoites were positive by qRT-PCR on day 7 (Figure 4C). Furthermore, parasites could be detected by Giemsa-stained thin blood smear within 1–5 days of *in vitro* culture. In one of two mice infected with 100,000 *Pf abcc2⁻* sporozoites, 25 parasite equivalents/mL were detected by qRT-PCR, which is close to the limit of detection of the assay (20 parasites/mL) (Figure 4C). However, no parasites could be detected in Giemsa-stained thick or thin smears from *in vitro* culture of blood transitioned from *Pf abcc2⁻*-infected mice for up to two weeks of culture. The five FRG NOD huHep mice infected with one million *Pf abcc2⁻* sporozoites were analyzed by qRT-PCR on days 7 and 8 postinfection. On day 8, all mice were euthanized, exsanguinated, and blood was transferred to *in vitro* culture. No parasite 18S rRNA was detected from any of the five mice on day 7. In one of five mice, 44 parasite equivalents/mL of blood was detected by qRT-PCR on day 8, whereas the remaining four mice remained negative (Figure 4C). No parasites could be detected by thick or thin Giemsa-stained blood smears from any of the cultured blood after four weeks of culture. Samples from *in vitro* culture were also analyzed by qRT-PCR every week for four weeks and no parasite nucleic acid could be detected. These results show that the severe early liver stage growth defect of *Pf abcc2⁻* that we observed in infected liver tissue completely abrogated the formation of infectious exoerythrocytic merozoites in an *in vivo* infection model.

Pf ABCC2 is dispensable for parasite growth under optimal culture conditions

To thoroughly analyze the potential role of *Pf* ABCC2 in asexual blood stage replication under different culture conditions, the parasitemias of *Pf abcc2⁻* clones 2F3 and 1G7 were compared to *Pf* NF54 parasites over three replication cycles with media supplemented with 5% serum and 0.25% Albumax. No significant difference in growth was observed between *Pf abcc2⁻* and *Pf* NF54 parasites, indicating that under optimal growth conditions, *Pf* ABCC2 is dispensable for asexual blood stage growth and replication (Figure 5A). To investigate whether *Pf* ABCC2 plays a role in parasite survival under conditions of nutrient and oxidative
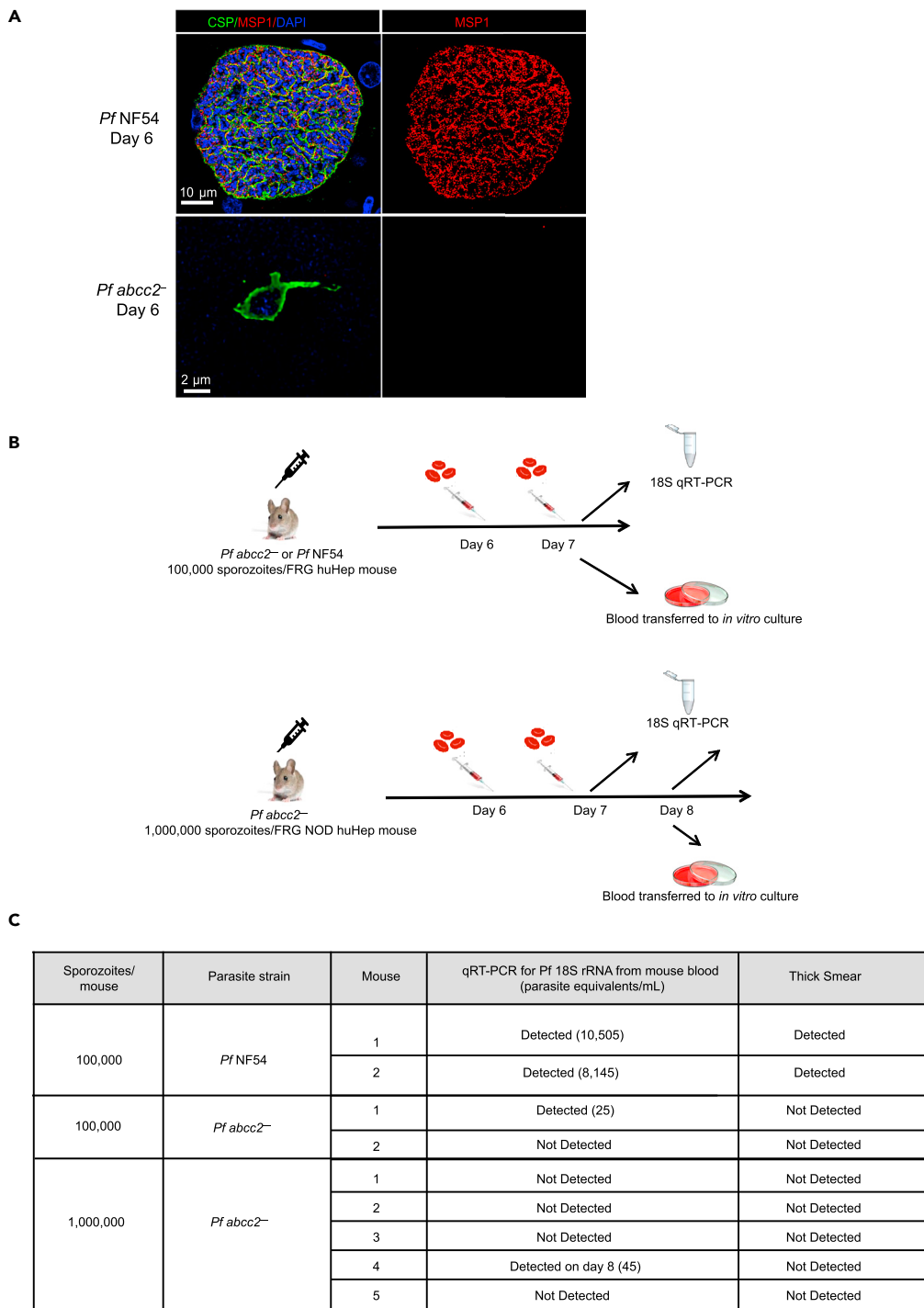
Figure 4. *Pf abcc2*⁻ liver stages do not form infectious exoerythrocytic merozoites

(A) Tissue sections were prepared from FRG huHep mice infected with one million sporozoites of either *Pf* NF54 or *Pf abcc2*⁻. On day 6 post sporozoite infection, liver stages were analyzed by IFA for expression of the PPM markers MSP1 (red) and CSP (green). DNA is stained with DAPI (blue). Scale bar size is 10 μm for *Pf* NF54 and 2 μm for *Pf abcc2*⁻.

(B) Schematics showing the experimental design of liver stage to blood stage transition experiments in humanized liver mice. Upper Panel: 100,000 sporozoites from *Pf* NF54 and *Pf abcc2*⁻ were injected into two FRG huHep mice, respectively. Mice were repopulated with human RBCs as depicted and 50 μL blood samples were collected from all mice for parasite 18S rRNA qRT-PCR samples on day 7. Two mice from each group infected with either *Pf* NF54 or *Pf abcc2*⁻ were

Figure 4. *Continued*

exsanguinated on day 7, and blood was transferred to *in vitro* culture and grown in culture for three weeks. Lower Panel: One million sporozoites from *Pf abcc2⁻* were injected into five FRG NOD huHep mice each. Mice were repopulated with human RBCs as depicted and 50 μL blood samples were collected from all mice for parasite 18S rRNA qRT-PCR samples on day 7 and 8. All five mice were exsanguinated on day 8, and blood was transferred to *in vitro* culture and grown in culture for six weeks.

(C) qPCR and blood smear analysis of transition experiments. Both mice infected with *Pf* NF54 were positive for *Pf* 18S rRNA by qRT-PCR and parasites could be detected by thick blood smears from the blood transferred to *in vitro* culture from the two mice. In one of two mice infected with *Pf abcc2*, 25 parasite equivalents/mL could be detected by qRT-PCR. The assay has a threshold detection cutoff of 20 parasite equivalents/mL. However, no parasites were detected by thick smear in the blood transitioned to *in vitro* culture for up to three weeks. One in five mice infected with one million sporozoites of *Pf abcc2⁻* was positive for *Pf* 18S rRNA on day 8 (44 parasite equivalents/mL). However, no parasites were detected in thick blood smears after six weeks of *in vitro* culture.

stress, we performed growth assays in which we did not change media over a period of two replication cycles and compared the parasitemia between *Pf abcc2⁻* and *Pf* NF54. Parasites were set up on day 0 at 0.25% parasitemia with media supplemented with 0.25% Albumax and 5% human serum. *Pf abcc2⁻* and *Pf* NF54 parasites grown under conditions of daily media change were used as controls. There was no significant difference in parasite growth between *Pf abcc2⁻* and *Pf* NF54 in the control group that received daily media change (Figure 5B). However, in the group that did not receive daily media change, there was a 2-fold reduction in parasitemia for the *Pf abcc2⁻* parasites as compared to *Pf* NF54 parasites after the second replication cycle, but this difference was not statistically significant.

To evaluate whether lack of ABCC2 results in a disadvantage when grown in competition with wild-type parasites, *Pf abcc2⁻* and *Pf* NF54 parasites were mixed in equal ratios and cultured together over nine consecutive replication cycles (Figure S3). Aliquots were removed every week during the competition experiment, extracted, and analyzed by qRT-PCR. No differences in relative abundance of *Pf abcc2⁻* and *Pf* NF54 parasites were detected, indicating that the wild-type parasites did not outcompete *Pf abcc2⁻* parasites.

DISCUSSION

Infectious *Plasmodium* salivary gland sporozoites are transmitted via mosquito bite and these sporozoites home to the liver and invade hepatocytes. Sporozoites prepare for hepatocyte infection by expression of proteins required for invasion, and by transcribing translationally repressed mRNAs that encode proteins which are involved in the establishment and modification of their intrahepatocytic niche (Lindner et al., 2019). During invasion, the parasite utilizes the hepatocyte plasma membrane to form a PV, which serves as the replication compartment for the nascent liver stage. Within the PV, the crescent-shaped intracellular sporozoite dedifferentiates into a spherical trophozoite, which is accompanied by extensive cellular remodeling and includes the dissolution of the invasive organelles and the inner membrane complex (Vaughan and Kappe, 2017). This prepares the early liver stage for entry into exoerythrocytic schizogony, which marks a transition point after which mobilization of host hepatocyte resources, which fuel the parasite's enormous cell expansion and genome replication becomes essential. Some molecular determinants of hepatocyte invasion, PV formation, and PV modification have been elucidated mostly in rodent malaria models (Vaughan and Kappe, 2017; Arredondo et al., 2018). However, proteins that are critical for the initiation of exoerythrocytic schizogony remain mostly unknown, particularly for human malaria parasites.

Here, we studied *Pf* ABCC2 expression and function using endogenously tagged protein, gene knockout, and a liver-humanized mouse model of infection. *Pf* ABCC2 was not expressed in *Pf* sporozoite stages. Our findings are corroborated by recent *Pf* salivary gland proteome data where no peptides for *Pf* ABCC2 could be detected in midgut or salivary gland sporozoites by mass spectrometry (Lindner et al., 2019). We observed that *Pf* ABCC2 expression is initiated during the early phases of liver stage development, as early as day 1 post infection and persists until mid-stage exoerythrocytic schizogony. We also show that this member of the ABCC family of transmembrane transporters localizes to the liver stage plasma membrane. *Pf* ABCC2 gene deletion resulted in a severe early liver stage developmental defect, as *Pf abcc2⁻* liver stages were arrested in development either in the transformation of sporozoites into trophozoites or at the onset of exoerythrocytic schizogony, which correlated with the onset of *Pf* ABCC2 protein expression. Although *Pf* ABCC2 was expressed in asexual stages, including trophozoites and schizonts, it was
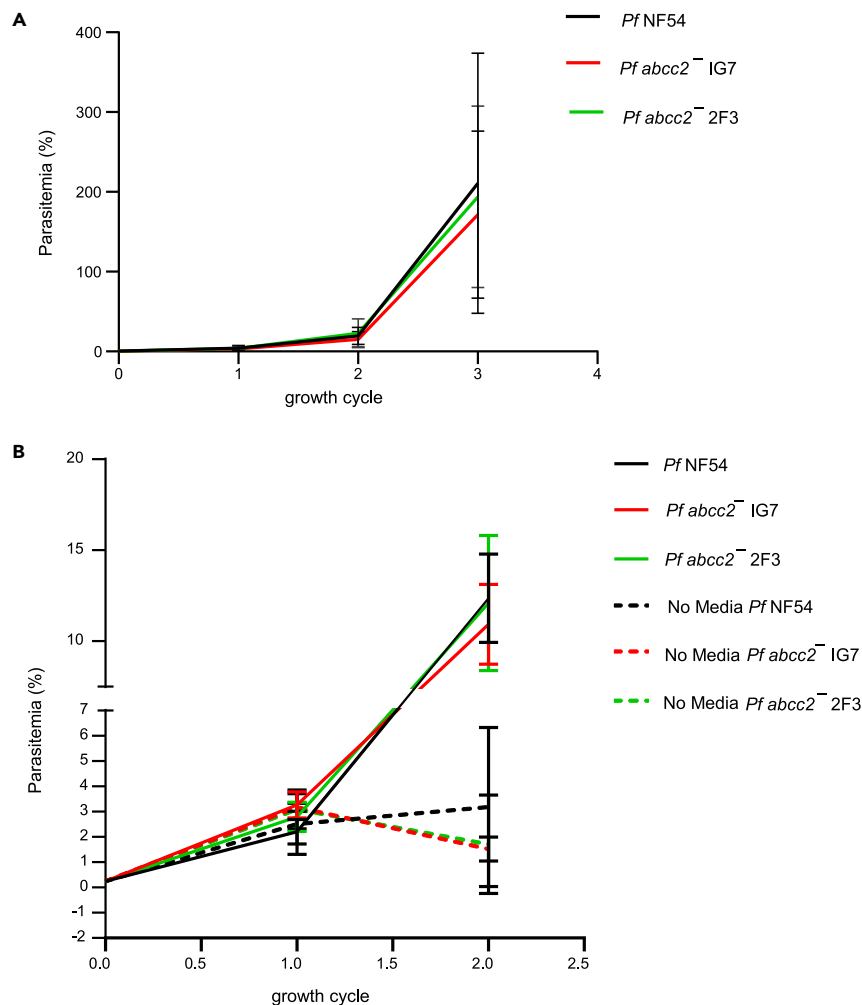
Figure 5. *Pf* ABCC2 is dispensable for intraerythrocytic growth under optimal media conditions but might play a role under conditions of stress

(A) Asexual blood stage parasitemia is compared between *Pf* NF54 (black line) and *Pf abcc2⁻* clones 1G7 (red line) and 2F3 (green line) over three replication cycles under optimal media conditions. Data are represented as mean $\pm$ SD, n = 3 biological replicates.

(B) Asexual blood stage parasitemia is compared between *Pf* NF54 (solid black line) and *Pf abcc2⁻* clones 1G7 (solid red line) and 2F3 (solid green line) under the conditions of daily media change and between *Pf* NF54 (dashed black line) and *Pf abcc2⁻* clones 1G7 (dashed red line) and 2F3 (dashed green line) under conditions of no media change for two replication cycles. Data are represented as mean $\pm$ SD, n = 3 biological replicates. Statistical analysis was carried out using two-way ANOVA.

dispensable for blood stage growth under optimum *in vitro* culture conditions. Interestingly, in contrast to the lack of *Pf* ABCC2 expression in sporozoites, we did detect its expression in erythrocytic merozoites.

A previous study of *Pf* ABCC2 using *in vitro* hepatocyte infections showed that it was expressed in replicating mid-to-late exoerythrocytic schizonts and gene-deficient-*Pf* ABCC2 parasites aborted growth in mid-to-late liver stage development (Rijpma et al., 2016). In contrast, our findings reported here, indicate that *Pf* ABCC2 is expressed in early-to-mid liver stages, and *Pf abcc2⁻* liver stages abort development at the transformation of sporozoites into trophozoites and at the trophozoite-to-schizont transition point. These differences in findings might be attributed to differences between an *in vitro* (primary human hepatocytes) used in the previous study (Rijpma et al., 2016) and the *in vivo* (liver humanized mice) model of liver stage development used here.

Using liver-humanized mice repopulated with human RBCs, we have demonstrated here that *Pf abcc2⁻* liver stages were unable to transition from the liver stage to the blood stage. No culturable asexual parasites could be recovered from humanized mice challenged with one million *Pf abcc2⁻* sporozoites, even after prolonged culture with RBCs. Nonetheless, in two of seven challenged mice, we could detect *Pf* 18S rRNA by a highly sensitive qRT-PCR diagnostic assay. Because *Pf abcc2⁻* liver stages persist in the liver at least until day 6, we speculate that the 18s rRNA signal detected in blood is likely originating from parasite nucleic acid (18S rRNA or genomic 18S rDNA) released from dying early liver stage-infected hepatocytes rather than from viable exoerythrocytic merozoites.

Multiple studies over the last decade have shown the efficacy of whole sporozoite-based vaccines against malaria (38–41). Targeted gene deletions enable generation of designed genetically attenuated parasites (GAP) that can arrest either early in liver stage development (replication-deficient) or late in liver stage development (replication-competent) (42–47). *Pf abcc2⁻* parasites undergo further liver stage development than what has been reported for the PfGAP3KO, a replication-deficient strain which carries deletions in the SAP1, P52, and P36 genes and that has been tested in humans (Kublin et al., 2017). Thus, it might be of interest to evaluate the *Pf abcc2⁻* parasites as a replication-deficient immunogen in humans.

Two hallmarks of liver stage development are the radical cellular transformation of intracellular sporozoites into trophozoites, followed by massive cell growth and genome replication during exoerythrocytic schizogony (Graewe et al., 2012; Vaughan and Kappe, 2017). High amounts of toxic oxidative by-products likely accumulate from the intense cellular reorganization and the metabolic turnover that might occur during these distinct development phases. These toxic metabolites would need to be actively exported from the parasite cytoplasm. Various *Plasmodium* membrane transporters have been identified that function at the parasite-host interface in the asexual stages to maintain redox homeostasis within the parasite (Koenderink et al., 2010; Martin, 2019). Because all eukaryotic ABC transporters are exporters, it is reasonable to hypothesize that the liver stage PPM-localized *Pf*ABCC2 actively exports toxic metabolites from the liver stage cytoplasm into the PV lumen. There is evidence that several members of the human ABCC transporter family play a critical role in maintaining redox homeostasis in the liver by secreting organic anions from the liver into bile (Liang and Aszalos, 2006). Mammalian ABCC transporters are known to export organic anions such as glutathione conjugates, glucuronide conjugates, and sulfate conjugates across biological membranes (Rebbeor et al., 2002; Cole and Deeley, 2006; Hollenstein et al., 2007; Jones and George, 2007; Zimmermann et al., 2008). *Pf* encodes two ABCC transporters, ABCC1 and ABCC2 (González-Pons et al., 2009; Koenderink et al., 2010). Although there are no known substrates for *Pf*ABCC2 studied here, there is evidence that *Pf*ABCC1 in the asexual stages, exports reduced glutathione (GSH) conjugates from the parasite cytoplasm into the host RBC (Raj et al., 2009). Based on the structural homology in the nucleotide binding domains of *Pf*ABCC1 and ABCC2, it is likely that GSH conjugates are also substrates for *Pf*ABCC2.

Polymorphisms and mutations in the *Pf ABCC* loci have been associated with drug resistance and changes in parasite fitness (Jones and George, 2007; Seeger and van Veen, 2009; Koenderink et al., 2010). Multiple studies have reported a role of *Pf ABCC1* in antimalarial drug resistance (Mu et al., 2003; Dahlström et al., 2009a, 2009b; Raj et al., 2009), and gene disruption of *Pf ABCC1* has been associated with reduced parasite fitness (Raj et al., 2009). Increased expression of *Pf ABCC2* has been reported to alter sensitivity to antimalarial drugs (Mok et al., 2014). Recently it was reported that polymorphisms and mutations in the *Pf ABCC2* allele might be associated with reduced parasite fitness in artemisinin-resistant *Pf* strains (Li et al., 2019). In this study we did not observe any loss of fitness in *Pf abcc2⁻* parasites under optimal cell culture conditions and when both *Pf abcc2⁻* and *Pf* NF54 wild-type strains were cultured together over prolonged periods of time. However, we observed a modest growth phenotype in *Pf abcc2⁻* parasites under conditions of severe nutrient and oxidative stress caused by the non-removal of spent media. This growth reduction might be caused by increased accumulation of toxic metabolites in the *Pf abcc2⁻* compared to *Pf* NF54 parasites, which in turn is caused by a lack of export of these metabolites out of the *Pf abcc2⁻* parasite cytoplasm. It has been previously reported that GSH-mediated heme detoxification in infected RBCs is crucial for parasite fitness (Meierjohann et al., 2002), and this regulation might be compromised in the *Pf abcc2⁻*. Nonetheless, we cannot completely rule out the possibility that *Pf*ABCC1 compensates for lack of *Pf*ABCC2 in the blood stages, and therefore we observed only modest blood stage growth defects in the *Pf abcc2⁻* parasites.

In conclusion, we have provided evidence that *Pf* ABCC2 marks the transition of invasive sporozoites to early intrahepatocytic *Pf* liver stage development. *Pf* ABCC2 is critical for successful parasite transition to exoerythrocytic schizogony, and its disruption results in complete loss of exoerythrocytic merozoite formation and blood stage infection in the liver-humanized mouse model.

Limitations of the study

The data shown in this manuscript does not address the possibility of a delay in release of *Pf abcc2⁻* parasites from the liver to blood or delayed growth of blood stage parasites originating from the liver. There are technical limitations for performing such an experiment. It requires the frequent administration of immunocompromised FRG huHep mice with clodronate liposomes and cyclophosphamide to deplete the innate immune cells such as macrophages and neutrophils, respectively. This treatment is required to prevent elimination of human RBCs by these innate immune cells in the spleen and ensures sustained repopulation of mouse blood with human RBCs. These repeated handlings increase the risk of mortality in the already immunocompromised FRG huHep mice and makes these mice much more susceptible to bacterial infections.

STAR★METHODS

Detailed methods are provided in the online version of this paper and include the following:

- KEY RESOURCES TABLE
- RESOURCE AVAILABILITY
  - Lead contact
  - Materials availability
  - Data and code availability
- EXPERIMENTAL MODEL AND SUBJECT DETAILS
  - Animals
  - *In vitro* culturing of *Pf* parasite lines
- METHOD DETAILS
  - Generation of *Pf abcc2⁻* and *Pf ABCC2^{mCherry}* parasites using CRISPR-Cas9-mediated gene editing
  - Parasite cloning by limiting dilution
  - Asexual growth kinetics assays
  - Measurement of competitive asexual blood stage growth between *Pf* NF54 and *Pf abcc2⁻* parasites
  - Gametocyte culture and mosquito infections
  - Phenotypic analysis of *Pf abcc2⁻* parasites in FRG-huHep mice
  - *Plasmodium* 18S rRNA qRT-PCR quantification of parasite load
  - Immunofluorescence assay of liver stage parasites
  - Immunofluorescence assay of blood stage parasites
  - Immunofluorescence assay of parasite mosquito stages
  - Microscopy
- QUANTIFICATION AND STATISTICAL ANALYSIS

SUPPLEMENTAL INFORMATION

Supplemental information can be found online at https://doi.org/10.1016/j.isci.2022.104224.

AUTHOR CONTRIBUTIONS

S.H.I.K., A.V., and D.G., conceived the work and designed experiments. D.G., S.K., W.B., J.A., M.H., and N.C. carried out laboratory work and collected and analyzed the data. C.P., A.M.S., and S.C.M. created and analyzed the qRT-PCR data and contributed to discussion. D.G., A.V., and S.H.I.K. wrote the manuscript.

DECLARATION OF INTERESTS

The authors declare no competing interests.

REFERENCES

Arredondo, S.A., Swearingen, K.E., Martinson, T., Steel, R., Dankwa, D.A., Harupa, A., Camargo, N., Betz, W., Vigdorovich, V., Oliver, B.G., et al. (2018). The micronemal plasmodium proteins P36 and P52 act in concert to establish the replication-permissive compartment within infected hepatocytes. Front. Cell. Infect. Microbiol. *8*, 413. https://doi.org/10.3389/fcimb.2018.00413.

Arredondo, S.A., Schepis, A., Reynolds, L., and Kappe, S.H.I. (2021). Parasitology secretory organelle function in the plasmodium sporozoite. Trends Parasitol. 1–13. https://doi.org/10.1016/j.pt.2021.01.008.

Azuma, H., Paulk, N., Ranade, A., Dorrell, C., Al-dhalimy, M., Ellis, E., Strom, S., Kay, M.A., Finegold, M., and Grompe, M. (2007). Robust expansion of human hepatocytes in Fah−/−/Rag2−/− Il2rg −/− mice. Nat. Biotechnol. *25*, 903–910. https://doi.org/10.1038/nbt1326.

Cole, S.P.C., and Deeley, R.G. (2006). Transport of glutathione and glutathione conjugates by MRP1. Trends Pharmacol. Sci. *27*. https://doi.org/10.1016/j.tips.2006.06.008.

Dahlström, S., Ferreira, P.E., Veiga, M.I., Sedighi, N., Wiklund, L., Mårtensson, A., Färnert, A., Sisowath, C., Osório, L., Darban, H., et al. (2009a). Plasmodium falciparum multidrug resistance protein 1 and artemisinin-based combination therapy in Africa. J. Infect. Dis. *200*, 1456–1464. https://doi.org/10.1086/606009.

Dahlström, S., Veiga, M.I., Mårtensson, A., Björkman, A., and Gil, J.P. (2009b). Polymorphism in Pfmrp1 (Plasmodium falciparum multidrug resistance protein 1) amino acid 1466 associated with resistance to sulfadoxine-pyrimethamine treatment. Antimicrob. Agents Chemother. *53*, 2553–2556. https://doi.org/10.1128/AAC.00091-09.

Draper, S.J., Sack, B.K., King, C.R., Nielsen, C.M., Rayner, J.C., Higgins, M.K., Long, C.A., and Seder, R.A. (2018). Malaria vaccines: recent advances and new horizons. Cell Host Microbe *24*, 43–56. https://doi.org/10.1016/j.chom.2018.06.008.

Duffy, P.E., and Gorres, J.P. (2020). Malaria vaccines since 2000: progress, priorities, products. NPJ Vaccines. *5*, 1–9. https://doi.org/10.1038/s41541-020-0196-3.

Foquet, L., Schafer, C., Minkah, N.K., Alanine, D.G.W., Flannery, E.L., Steel, R.W.J., Sack, B.K., Camargo, N., Fishbaugher, M., Betz, W., et al. (2018). Plasmodium falciparum liver stage infection and transition to stable blood stage infection in liver-humanized and blood-humanized FRGN KO mice enables testing of blood stage inhibitory antibodies (reticulocyte-binding protein homolog 5) in vivo. Front.

Immunol. *9*, 1–8. https://doi.org/10.3389/fimmu.2018.00524.

González-Pons, M., Szeto, A.C., González-Méndez, R., and Serrano, A.E. (2009). Identification and bioinformatic characterization of a multidrug resistance associated protein (ABCC) gene in Plasmodium berghei. Malar. J. *8*, 1–13. https://doi.org/10.1186/1475-2875-8-1.

Goswami, D., Betz, W., Locham, N.K., Parthiban, C., Brager, C., Schäfer, C., Camargo, N., Nguyen, T., Kennedy, S.Y., Murphy, S.C., et al. (2020). A replication-competent late liver stage-attenuated human malaria parasite. JCI Insight *5*. https://doi.org/10.1172/jci.insight.135589.

Graewe, S., Stanway, R.R., Rennenberg, A., and Heussler, V.T. (2012). Chronicle of a death foretold: plasmodium liver stage parasites decide on the fate of the host cell. FEMS Microbiol. Rev. *36*, 111–130. https://doi.org/10.1111/j.1574-6976.2011.00297.x.

Hodgson, S.H., Douglas, A.D., Edwards, N.J., Kimani, D., Elias, S.C., Chang, M., Daza, G., Seilie, A.M., Magiri, C., Muia, A., et al. (2015). Increased sample volume and use of quantitative reverse-transcription PCR can improve prediction of liver-to-blood inoculum size in controlled human malaria infection studies. Malar. J. *14*, 1–9. https://doi.org/10.1186/s12936-015-0541-6.

Hollenstein, K., Dawson, R.J., and Locher, K.P. (2007). Structure and mechanism of ABC transporter proteins. Curr. Opin. Struct. Biol. *17*, 412–418. https://doi.org/10.1016/j.sbi.2007.07.003.

Ishino, T., Chinzei, Y., and Yuda, M. (2005). Two proteins with 6-cys motifs are required for malarial parasites to commit to infection of the hepatocyte. Mol. Microbiol. *58*, 1264–1275. https://doi.org/10.1111/j.1365-2958.2005.04801.x.

Jobe, O., Lumsden, J., Mueller, A., Williams, J., Silva-Rivera, H., Kappe, S.H.I., Schwenk, R.J., Matuschewski, K., and Krzych, U. (2007). Genetically attenuated Plasmodium berghei liver stages induce sterile protracted protection that is mediated by major histocompatibility complex class I–dependent interferon-γ–producing CD8^{+} T cells. J. Infect. Dis. *196*, 599–607. https://doi.org/10.1086/519743.

Jones, P.M., and George, A.M. (2007). Multidrug resistance in parasites : ABC transporters , P-glycoproteins and molecular modelling. Int. J. Parasitol. *35*, 555–566. https://doi.org/10.1016/j.ijpara.2005.01.012.

Kappe, S.H., Gardner, M.J., Brown, S.M., Ross, J., Matuschewski, K., Ribeiro, J.M., Adams, J.H., Quackenbush, J., Cho, J., Carucci, D.J., et al. (2001). Exploring the transcriptome of the malaria

sporozoite stage. Proc. Natl. Acad. Sci. U S A. *98*, 9895–9900. https://doi.org/10.1073/pnas.171185198.

Koenderink, J.B., Kavishe, R.A., Rijpma, S.R., and Russel, F.G.M. (2010). The ABCs of multidrug resistance in malaria. Trends Parasitol. *26*, 440–446. https://doi.org/10.1016/j.pt.2010.05.002.

Kreutzfeld, O., Müller, K., and Matuschewski, K. (2017). Engineering of genetically arrested parasites (GAPs) for a precision malaria. Vaccine *7*, 1–13. https://doi.org/10.3389/fcimb.2017.00198.

Kublin, J.G., Mikolajczak, S.A., Sack, B.K., Fishbaugher, M.E., Seilie, A., Shelton, L., VonGoedert, T., Firat, M., Magee, S., Fritzen, E., et al. (2017). Complete attenuation of genetically engineered Plasmodium falciparum sporozoites in human subjects. Sci. Transl. Med. *9*, 1–12. https://doi.org/10.1126/scitranslmed.aad9099.

Labaied, M., Harupa, A., Dumpit, R.F., Coppens, I., Mikolajczak, S.A., and Kappe, S.H.I. (2007). Plasmodium yoelii sporozoites with simultaneous deletion of P52 and P36 are completely attenuated and confer sterile immunity against infection. Infect. Immun. *75*, 3758–3768. https://doi.org/10.1128/IAI.00225-07.

Li, X., Kumar, S., Mcdew-white, M., Haile, M., Cheeseman, I.H., Emrich, S., Button-Simons, K., Nosten, F., Kappe, S.H.I., Ferdig, M.T., et al. (2019). Genetic mapping of fitness determinants across the malaria parasite Plasmodium falciparum life cycle. PLoS Genet. *15*, e1008453.

Liang, X., and Aszalos, A. (2006). Multidrug transporters as drug targets. Curr. Drug Targets, 911–921.

Lindner, S.E., Swearingen, K.E., Shears, M.J., Walker, M.P., Vrana, E.N., Hart, K.J., Minns, A.M., Sinnis, P., Moritz, R.L., and Kappe, S.H.I. (2019). Transcriptomics and proteomics reveal two waves of translational repression during the maturation of malaria parasite sporozoites. Nat. Commun. *10*, 1–13. https://doi.org/10.1038/s41467-019-12936-6.

Loubens, M., Vincensini, L., Fernandes, P., Briquet, S., Marinach, C., and Silvie, O. (2020). Plasmodium sporozoites on the move: switching from cell traversal to productive invasion of hepatocytes. Mol. Microbiol. 1–12. https://doi.org/10.1111/mmi.14645.

MacKellar, D.C., O'Neill, M.T., Aly, A.S.I., Sacci, J.B., Cowman, A.F., and Kappe, S.H.I. (2010). Plasmodium falciparum PF10_0164 (ETRAMP10.3) is an essential parasitophorous vacuole and exported protein in blood stages.

Eukaryot. Cell *9*, 784–794. https://doi.org/10.1128/EC.00336-09.

Marin-mogollon, C., Salman, A.M., Koolen, K.M.J., and Bolscher, J.M. (2019). A P . falciparum NF54 reporter line expressing mCherry-luciferase in gametocytes , sporozoites , and liver-stages. Front. Cell. Infect. Microbiol. *9*, 1–13. https://doi.org/10.3389/fcimb.2019.00096.

Martin, R.E. (2019). The transportome of the malaria parasite. Biol. Rev. *8*. https://doi.org/10.1111/brv.12565.

Medica, D.L., and Sinnis, P. (2005). Quantitative dynamics of plasmodium yoelii sporozoite transmission by infected anopheline Mosquitoes. Infect Immun. *73*, 4363–4369. https://doi.org/10.1128/IAI.73.7.4363.

Meierjohann, S., Walter, R.D., and Müller, S. (2002). Regulation of intracellular glutathione levels in erythrocytes infected with chloroquine-sensitive and chloroquine-resistant Plasmodium falciparum. Biochem. J. *368*, 761–768. https://doi.org/10.1042/BJ20020962.

Mikolajczak, S.A., Lakshmanan, V., Fishbaugher, M., Camargo, N., Harupa, A., Kaushansky, A., Douglass, A.N., Baldwin, M., Healer, J., O'Neill, M., et al. (2014). A next-generation genetically attenuated Plasmodium falciparum parasite created by triple gene deletion. Mol. Ther. J. Am. Soc. Gene Ther. *22*, 1707–1715. https://doi.org/10.1038/mt.2014.85.

Mok, S., Liong, K.Y., Lim, E.H., Huang, X., Zhu, L., Preiser, P.R., and Bozdech, Z. (2014). Structural polymorphism in the promoter of pfmrp2 confers Plasmodium falciparum tolerance to quinoline drugs. Mol. Microbiol. *91*, 918–934. https://doi.org/10.1111/mmi.12505.

Mu, J., Ferdig, M.T., Feng, X., Joy, D.A., Duan, J., Furuya, T., Subramanian, G., Aravind, L., Cooper, R.A., Wootton, J.C., et al. (2003). Multiple transporters associated with malaria parasite responses to chloroquine and quinine. Mol. Microbiol. *49*, 977–989. https://doi.org/10.1046/j.1365-2958.2003.03627.x.

Mueller, A.-K., Camargo, N., Kaiser, K., Andorfer, C., Frevert, U., Matuschewski, K., and Kappe, S.H.I. (2005a). Plasmodium liver stage developmental arrest by depletion of a protein at the parasite-host interface. Proc. Natl. Acad. Sci. U.S.A. *102*, 3022–3027. https://doi.org/10.1073/pnas.0408442102.

Mueller, A., Labaied, M., Kappe, S.H.I., and Matuschewski, K. (2005b). Genetically modified Plasmodium parasites as a protective experimental malaria vaccine. Nature *433*, 164–167.

Raj, D.K., Mu, J., Jiang, H., Kabat, J., Singh, S., Sullivan, M., Fay, M.P., Mccutchan, T.F., and Su, X. (2009). Disruption of a plasmodium falciparum multidrug resistance-associated protein (PfMRP)

alters its fitness and transport of antimalarial drugs and glutathione. J. Biol. Chem. *284*, 7687–7696. https://doi.org/10.1074/jbc.M806944200.

Rebbeor, J.F., Connolly, G.C., and Ballatori, N. (2002). Inhibition of Mrp2- and Ycf1p-mediated transport by reducing agents : evidence for GSH transport on rat Mrp2. Biochim. Biophys. Acta *1559*, 171–178.

Rijpma, S.R., Van Der Velden, M., Gonzalez-Pons, M., Annoura, T., van Schaijk, B.C.L., van Gemert, G.-J., van den Heuvel, J.M.W., Ramesar, J., Chevalley-Maurel, S.C., et al. (2016). Multidrug ABC transporters are essential for hepatic development of Plasmodium sporozoites. Cell Microbiol. *18*, 369–383. https://doi.org/10.1186/s40945-017-0033-9.Using.

Sack, B.K., Mikolajczak, S.A., Fishbaugher, M., Vaughan, A.M., Flannery, E.L., Nguyen, T., Betz, W., Jane Navarro, M., Foquet, L., Steel, R.W.J., et al. (2017). Humoral protection against mosquito bite-transmitted Plasmodium falciparum infection in humanized mice. NPJ Vaccines *2*, 1–10. https://doi.org/10.1038/s41541-017-0028-2.

Schäfer, C., Roobsoong, W., Kangwanrangsan, N., Bardelli, M., Rawlinson, T.A., Dambrauskas, N., Trakhimets, O., Parthiban, C., Goswami, D., Reynolds, L.M., et al. (2020). A humanized mouse model for plasmodium vivax to test interventions that block liver stage to blood stage transition and blood stage infection. iScience *23*. https://doi.org/10.1016/j.isci.2020.101381.

Seeger, M.A., and van Veen, H.W. (2009). Molecular basis of multidrug transport by ABC transporters. Biochim. Biophys. Acta *1794*, 725–737. https://doi.org/10.1016/j.bbapap.2008.12.004.

Seilie, A.M., Chang, M., Hanron, A.E., Billman, Z.P., Stone, B.C., Zhou, K., Olsen, T.M., Daza, G., Ortega, J., Cruz, K.R., et al. (2019). Beyond blood smears: qualification of plasmodium 18s rrna as a biomarker for controlled human malaria infections. Am. J. Trop. Med. Hyg. *100*, 1466–1476. https://doi.org/10.4269/ajtmh.19-0094.

Tarun, A.S., Dumpit, R.F., Camargo, N., Labaied, M., Liu, P., Takagi, A., Wang, R., and Kappe, S.H.I. (2007). Protracted sterile protection with *Plasmodium yoelii* pre-erythrocytic genetically attenuated parasite malaria vaccines is independent of significant liver-stage persistence and is mediated by CD8 [+] T cells. J. Infect. Dis. *196*, 608–616. https://doi.org/10.1086/519742.

Upton, D.C., Gregory, B.L., Arya, R., and Unniraman, S. (2011). ABC transporters: a riddle wrapped in a mystery inside an enigma. Immunol. Res. *49*, 14–24. https://doi.org/10.1007/s12026-010-8190-x.

van Dijk, M.R., Douradinha, B., Franke-Fayard, B., Heussler, V., van Dooren, M.W., van Schaijk, B., van Gemert, G.-J., Sauerwein, R.W., Mota, M.M.,

Waters, A.P., et al. (2005). Genetically attenuated, P36p-deficient malarial sporozoites induce protective immunity and apoptosis of infected liver cells. Proc. Natl. Acad. Sci. U S A. *102*, 12194–12199. https://doi.org/10.1073/pnas.0500925102.

Vanbuskirk, K.M., O'Neill, M.T., De la Vega, P., Maier, A.G., Krzych, U., Williams, J., Dowler, M.G., Sacci, J.B., Kangwanrangsan, N., Tsuboi, T., et al. (2009). Preerythrocytic, live-attenuated Plasmodium falciparum vaccine candidates by design. Proc. Natl. Acad. Sci. U S A. *106*, 13004–13009.

Vaughan, A.M., Mikolajczak, S.A., Wilson, E.M., Grompe, M., Kaushansky, A., Camargo, N., Bial, J., Ploss, A., and Kappe, S.H.I. (2012). Technical advance Complete Plasmodium falciparum liver-stage development in liver-chimeric mice. J. Clin. Invest. *122*. https://doi.org/10.1172/JCI62684.3618.

Vaughan, A.M., Pinapati, R.S., Cheeseman, I.H., Camargo, N., Fishbaugher, M., Checkley, L.A., Nair, S., Hutyra, C.A., Nosten, F.H., Anderson, T.J.C., et al. (2015). Plasmodium falciparum genetic crosses in a humanized mouse model. Nat. Methods *12*, 631–633. https://doi.org/10.1038/nmeth.3432.

Vaughan, A.M., Kappe, S.H.I., Vaughan, A.M., and Genetically, S.H.I.K. (2017). Expert Review of Vaccines Genetically attenuated malaria parasites as vaccines. Expert Rev. Vaccin. *16*, 765–767. https://doi.org/10.1080/14760584.2017.1341835.

Vaughan, A.M., and Kappe, S.H.I. (2017). Malaria Parasite Liver Infection and Exoerythrocytic Biology. Cold Spring Harbor Laboratory Med. *7*. https://doi.org/10.1101/cshperspect.a025486.

Walther, M., Dunachie, S., Keating, S., Vuola, J.M., Berthoud, T., Schmidt, A., Maier, C., Andrews, L., Andersen, R.F., Gilbert, S., et al. (2005). Safety, immunogenicity and efficacy of a pre-erythrocytic malaria candidate vaccine, ICC-1132 formulated in Seppic ISA 720. Vaccine *23*, 857–864. https://doi.org/10.1016/j.vaccine.2004.08.020.

Wilkens, S. (2015). Structure and mechanism of ABC transporters. F1000Prime Rep. *7*, 1–9. https://doi.org/10.12703/P7-14.

World Health Organization, W (2021). World Malaria Report 2021 (World Health Organization).

Zimmermann, C., Van De Wetering, K., Van De Steeg, E., Wagenaar, E., Vens, C., and Schinkel, A.H. (2008). Species-dependent transport and modulation properties of human and mouse multidrug resistance protein 2 (MRP2/Mrp2, ABCC2/Abcc2). Drug Metab. Dispos. *36*, 631–640. https://doi.org/10.1124/dmd.107.019620.

STAR★METHODS

KEY RESOURCES TABLE

REAGENT or RESOURCE	SOURCE	IDENTIFIER
Antibodies		
Anti-*P.falciparum* CSP	BEI Resources	BEI-MRA-183A clone 2A10
Anti-*P.vivax* BiP (immunoglobulin-binding protein)	Stefan H.I. Kappe	polyclonal
Anti-*P. yoeli* ACP (Acyl Carrier Protein)	Stefan H.I. Kappe	clone 40001
Anti-*P. vivax* mitochondrial HSP70	Stefan H.I. Kappe	Rabbit polyclonal
Anti- *P.falciparum* MSP-1	European Malaria Reagent Repository	clone 12.10
Anti-*Pf* Exp1	Gift from Klaus Lingelbach	Rabbit polyclonal sera
Anti-mCherry	Thermo Fischer	Cat# M11217 clone 16D7; RRID: AB_2536611
Donkey anti-mouse 488	Invitrogen	Cat # A21202; RRID: AB_141607
Donkey anti-mouse 594	Invitrogen	Cat # A21203; RRID: AB_141633
Donkey anti-mouse 647	Invitrogen	Cat # A31571; RRID: AB_162542
Donkey anti-rabbit 488	Invitrogen	Cat # A21206; RRID: AB_2535792
Donkey anti-rabbit 594	Invitrogen	Cat # A21207; RRID: AB_141637
Donkey anti-rabbit 647	Invitrogen	Cat # A31573; RRID: AB_2536183
Biological samples		
P.falciparum NF54	Walter Reed Army Institute of Research (WRAIR)	MBR-0004, Lot Number A004 produced at Seattle Biomed from WRAIR Lot Number 0148
P.falciparum abcc2⁻	This Manuscript	N/A
P.falciparum ABCC2^{mCherry}	This Manuscript	N/A
Chemicals, peptides, and recombinant proteins		
RPMI 1640 media containing hypoxanthine, sodium bicarbonate, and 4-(2-hydroxyethyl)-1-piperazineethanesulfonic acid	Invitrogen™ (custom made)	Project No: PB11096
Human Serum	Valley Biomedical	Cat # HS1004
AlbuMAX™ II Lipid-Rich BSA	Thermo Fischer	Cat # 11021029
Gentamicin (10 mg/mL)	Invitrogen™	Cat # 15710064
O+ human blood	Valley Biomedical	Cat # 10020
WR99210	Jacobus Pharmaceuticals	N/A
NucliSENS lysis buffer	bioMérieux, Marcy-l'Étoile, France	Cat # 280134
Paraformaldehyde, 16% w/v aq. soln., methanol free	Alfa Aesar	Cat # 43368-9M
Schneider's Drosophila Medium	Gibco™	Cat # 21720024
4-,6- diamidino-2-phenylindole (DAPI)	Thermo Fischer	Cat # D1306
ProLong™ Gold Antifade Mountant	Invitrogen™	Cat # P36930
4-Aminobenzoic acid (p-aminobenzoic acid or pABA)	Aldrich	Cat #100336
Heparin (sodium salt from porcine intentinal mucosa)	Sigma-Aldrich	Cat # H5515-100KU
Potassium permanganate		
Methanol	VWR	Cat # BDH1135-4LG
Fluriso™ (Isoflurane, USP)	Vet One	Cat # 502,017
1 kb Ladder	Promega	Cat # G5711

Continued

REAGENT or RESOURCE	SOURCE	IDENTIFIER
Experimental models: Organisms/strains		
Mouse: FRG® KO on C57Bl/6—Human Repopulated, 70%+	Yecuris™	Cat # 10-0006
Mouse: FRG® KO on NOD—Human Repopulated, 70%+	Yecuris™	Cat # 10-0013
Oligonucleotides (restrictions sites are underlined and overhangs are in italics)		
Primers for *Pf abcc2* generation (restrictions sites are underlined and overhangs are in italics):		
ABCC2_5′flank_F 5′-TATA<u>CTCGAG</u>ATATTGAGCATCTGTTTAT ACATTG-3′	IDT	N/A
ABCC2_5′flank_R 5′-CCAAGCTAGCTATAGGCGCGCCTAAAAA CGGAATCTTTCTAACTTTACT-3′	IDT	N/A
ABCC2_3′flank_F 5′-AGGCGCGCCTATAGCTAGCTTGGGAAAA ACAATTAAATTG-3′	IDT	N/A
ABCC2_3′flank_R 5′-TATA<u>CTCGAG</u>TTGTTAAAAAAGTTACCTG AATTGTTC-3′	IDT	N/A
ABCC2_guide1 F 5′-*tatt*GGCCCTTTCCCTCTTCACTA-3′	IDT	N/A
ABCC2_guide1 R 5′-*aaac*TAGTGAAGAGGGAAAGGGCC-3′	IDT	N/A
Genotyping_P1 5′-GGTATCGTAGGAAAATCAGG-3′	IDT	N/A
Genotyping_P2 5′-GTATACAACTTCTCCCTTTGCG-3′	IDT	N/A
Genotyping_P3 5′-AGGCGCGCCTATACCCGGGTTGG-3′	IDT	N/A
Genotyping_P4 5′-GCATGAATGGTTCATGC-3′	IDT	N/A
Primers for *Pf ABCC2^{mcherry}* generation (restrictions sites are underlined and overhangs are in italics):	IDT	N/A
5′mCherry ABCC2_R 5′-*tcttcttctcctttgaaac*ATTTA ATTGTTTTTCTTGAAGCAAGTTAGCCAACTCTG TTTGTGTTTTAACATCTTTATAACTAC-3′	IDT	N/A
3′mCherryABCC2_F 5′-ATT<u>GCGGCCGCG</u>AGTGAGTTTATGT ATATAATGTGTATATC-3′	IDT	N/A
3′mCherry ABCC2_R5′ AAAC<u>GAATTC</u>GTTAAAAAAGTTACCT GAATTGTTC 3′	IDT	N/A
ABCC2_guide3 F 5′-*tatt*TTGAAGCAAGTTAGCTAATT-3′	IDT	N/A
ABCC2_guide3 R 5′-*aaac*AATTAGCTAACTTGCTTCAA-3′	IDT	N/A
ABCC2_ORF_F_genotyping_P4 5′-GGTATCGTAGGAAAAT CAGG-3′	IDT	N/A
mCherry_rev_genotyping_P5 5′-CCACCAGTACTATGTCTTCC-3′	IDT	N/A
Primers for blood stage competition assay genotyping primers: *Pf abcc2* primers: Linker_F 5′-CGCGCCTATAGCTAGCTTG-3′ ABCC_3UTR_R 5′-CCCTTTCCAATATAGGCGTTC-3′ *Pf NF54* primers ABCC_ORF_F 5′GCATCACATGCACCCTTATG-3′ ABCC_ORF_R 5′AGAAGGTTAGCGCCAGAACA-3′	IDT	N/A
Primer for screening *Pf* serial dilutions: 18SF (5′-AACCTGGTTGA TCCAGTAGTCATATG-3′)	IDT	N/A
Primer for screening *Pf* serial dilutions: 18SR (5′-CCAAAAATTG GCCTTGCATTGTTAT-3′)	IDT	N/A

Continued

REAGENT or RESOURCE	SOURCE	IDENTIFIER
Recombinant DNA		
Plasmid: p-ABCC2KO	This manuscript (modified from Goswami et al., 2020)	N/A
Plasmid: pFC-ABCC2-mCherry	This manuscript (modified from Goswami et al., 2020)	N/A
Software and algorithms		
Adobe Illustrator	Adobe	Adobe Illustrator 2020 https://www.adobe.com/products/illustrator.html
GraphPad Prism	GraphPad Prism Software	GraphPad Prism 9.2.0.332 https://www.graphpad.com/scientific-software/prism/ RRID: SCR_002798
Lightning software	Leica Microsystems	https://www.leica-microsystems.com/products/confocal-microscopes/p/leica-tcs-sp8/
Geneious®	Biomatters Ltd.	Geneious® 11.1.4 https://www.geneious.com/resources/
Biorender.com		https://biorender.com/

RESOURCE AVAILABILITY

Lead contact

Further information and requests for resources and reagents should be directed to and will be fulfilled by the Lead Contact, Stefan H.I. Kappe (Stefan.Kappe@seattlechildrens.org).

Materials availability

Plasmids and transgenic *Plasmodium falciparum* strains generated in the study are available upon request from the Lead contact with a material transfer agreement.

Data and code availability

- All data reported in this paper will be shared by the lead contact upon request.

- This paper does not report original code.

- Any additional information required to reanalyze the data reported in this paper is available from the lead contact upon request.

EXPERIMENTAL MODEL AND SUBJECT DETAILS

Animals

Study approval

This study was carried out in accordance with the recommendations of the NIH Office of Laboratory Animal Welfare standards (OLAW welfare assurance #D16-00119). Mice were maintained and bred under specific pathogen-free conditions at the Center for Global Infectious Disease Research, Seattle Children's Research Institute. The protocol was approved by the Center for Infectious Disease Research Institutional Animal Care and Use Committee (IACUC) under protocol 00480.

Mice. Female FRG and FRG NOD KO huHep mice, over 4 months of age were purchased from Yecuris Inc. In our previous studies, we have shown that both male and female genders of FRG and FRG NOD KO huHep mice can be used for *Plasmodium* sporozoite infection (Vaughan et al., 2015; Sack et al., 2017) and female mice were used in this study as also previously reported (Vaughan et al., 2012; Schäfer et al., 2020). Serum albumin levels of all mice used exceeded 4 mg/mL, corresponding to >70% human hepatocyte repopulation. Mice were maintained on drinking water containing 3% Dextrose and were cycled on 8 mg/L NTBC once a month for 4 days to maintain hepatocyte chimerism.

In vitro culturing of *Pf* parasite lines

Pf WT NF54, *Pf abcc2⁻* and *Pf ABCC2^mcherry^* were cultured in custom-made RPMI 1640 media containing hypoxanthine, sodium bicarbonate, and 4-(2-hydroxyethyl)-1-piperazineethanesulfonic acid (Invitrogen, Life Technologies, Grand Island, NY) supplemented with 5% human serum (Valley Biomedical) and 5% albumax (Invitrogen, Life Technologies, Grand Island, NY) and gentamycin (Invitrogen), in presence of O+ blood (Valley Biomedical) at 3–5% hematocrit, in an atmosphere of 5% CO$_2$, 5% O$_2$, and 90% N$_2$.

METHOD DETAILS

Generation of *Pf abcc2⁻* and *Pf ABCC2^mCherry^* parasites using CRISPR-Cas9-mediated gene editing

All oligonucleotides used for generating transgenic parasite strains are mentioned in detail in the STAR Methods. The CRISPR-Cas9 vector and gene targeting strategy have been previously described (Goswami et al., 2020). The p-ABCC2KO plasmid was generated by cloning the 5′ and-3′ homology arms flanking the *Pf ABCC2* gene into the pFC vector followed by cloning the guide RNA sequence. 5% sorbitol synchronized ring stage *Pf* NF54 parasites at 5–8% parasitemia were electroporated with 100 μg of p-ABCC2KO plasmid at 0.31 kV and 950 μF using a BioRad Gene Pulser (BioRad, Hercules, CA). Positive selection with 8 nM WR99210 (WR; Jacobus Pharmaceuticals, Princeton, NJ) was administered 24 h after the transfection and kept for five days. Drug resistant parasites were rescued after 21 days. These parasites were screened by PCR using primers P1 and P2 that bind inside the open reading frame and give a PCR amplicon only for the wildtype locus of *Pf ABCC2* and primers P3 and P4 that give a PCR amplicon only in the recombinant allele.

*Pf ABCC2^mCherry^* parasites were generated via CRISPR/Cas9-mediated gene editing as described above. pFC-ABCC2-mCherry plasmid was generated using the pFC-mCherry vector backbone, into which the 5′ homology arm amplified from within the open reading frame and carrying non-synonymous mutations in the guide sequence, 3′ homology arm and guide RNA were cloned. *Pf* NF54 parasites were transfected with 100 μg of the pFC-ABCC2-mCherry plasmid in the pFC plasmid backbone. Transfected parasites were positively selected as mentioned above, recombinant parasites were screened up PCR using primers P5 and P3 and cloned by limiting dilution.

Parasite cloning by limiting dilution

Pf abcc2⁻ and *Pf ABCC2^mCherry^* parasites were cloned out of the mixed parasite pool by limiting dilution in 96-well flat bottomed plates (Mikolajczak et al., 2014). Cultures were serially diluted and then plated at a density of 0.3 parasites per well in a 100μL volume at 2% hematocrit. Cultures were fed once a week and fresh blood was added every three – four days at 0.3% hct. The wells were screened for presence of *Plasmodium* 18S RNA parasites on day 18 using primers 18SF (5′-AACCTGGTTGATCCAGTAGTCATATG-3′) and 18SR (5′-CCAAAAATTGGCCTTGCATTGTTAT-3′). The positive wells were expanded and screened for recombination using the PCR strategies mentioned earlier.

Asexual growth kinetics assays

Under optimal media conditions between *Pf* NF54 wildtype and *Pf abcc2⁻*

Ring stage parasites of *Pf* NF54 WT and *Pf abcc2⁻* were set up at 0.5% parasitemia and 3% hematocrit in media containing 5% Albumax and 0.25% human serum. Fresh media was repleted daily. Growth was monitored over three replication cycles by making thin blood smeared every other day. Cultures were cut back by 3 – 5 folds after the second replication cycle to prevent parasite cultures from crashing. The parasitemia after the third replication cycle was calculated by multiplying the parasitemia based on blood smear with the diluted fold change.

Under conditions of no media change *Pf* NF54 wildtype and *Pf abcc2⁻*

Ring stage parasites of *Pf* NF54 WT and *Pf abcc2⁻* were set up at 0.25% parasitemia and 3% hematocrit in media containing 0.25% Albumax and 5% human serum. No fresh media was given throughout the duration of the experiment of two replication cycles or 4 days, but flasks were gassed daily. *Pf* NF54 wildtype and *Pf abcc2⁻* grown under the same media change and with daily media change were used as controls. Growth was monitored over two replication cycles by making thin blood smear every other day.

Between Pf NF54 wildtype and Pf ABCC2^mCherry

Ring stage parasites of *Pf* NF54 WT and *Pf ABCC2mCherry* were set up at 0.25% parasitemia and 3% hematocrit in media containing 0.25% Albumax and 5% human serum. Fresh media was repleted daily. Growth was monitored over three replication cycles by making thin blood smeared every other day. The parasitemia after the third replication cycle was calculated by multiplying the parasitemia based on blood smear with the diluted fold change.

Measurement of competitive asexual blood stage growth between *Pf* NF54 and *Pf abcc2*⁻ parasites

To compare competitive asexual blood stage replication and growth between the *Pf* NF54 and *Pf abcc2*⁻ parasites, synchronized parasites at ring stages were mixed in equal ratio at 0.5% parasitemia each for *Pf* NF54 and *Pf abcc2*⁻. These mixed parasites were cultured *in vitro*, and bulk parasite samples were collected every other day for nine replication cycles. Bulk parasites were utilized to extract genomic DNA and set up quantitative PCR using primers specific to *Pf NF54* wildtype or *Pfabcc2*⁻.

Gametocyte culture and mosquito infections

Pf WT NF54, *Pf abcc2*⁻ and *Pf ABCC2^mcherry* cultures were grown in gametocyte media containing RPMI 1640 media containing hypoxanthine, sodium bicarbonate, and 4-(2-hydroxyethyl)-1-piperazineethanesulfonic acid (Invitrogen, Life Technologies, Grand Island, NY) supplemented with 10% human serum (Valley Biomedical) in presence of O+ blood (Valley Biomedical) at 4% hematocrit, in an atmosphere of 5% CO_2, 5% O_2, and 90% N_2. Gametocyte cultures were initiated at 4% hematocrit and 0.8–1% parasitemia (mixed stages) and maintained for up to 15 days with daily medium changes. On days 15–17 post set up, stage V gametocytemia was evaluated by Giemsas-stained thin blood smears. Mature gametocyte cultures were spun down at 800 g for 2 min at 37°C to pellet infected RBCs. A volume of pre-warmed 100% human serum equal to the packed RBC volume was added to resuspend the RBC pellet. The resuspended pellet was diluted to a gametocytemia of 0.4–0.5% with pre-warmed feeding media containing 50% human serum and 50% human RBC and immediately fed to non–blood fed adult female *Anopheles stephensi* mosquitoes 3 to 7 days after hatching by membrane feeding assay. Mosquitoes were allowed to feed through Parafilm for up to 20 min. Following blood feeding, mosquitoes were maintained for up to 19 days at 27°C, 75% humidity, and provided with 8% dextrose solution in PABA water. Oocyst prevalence was checked on day 7–9 post feed by microdissecting approximately 12 midguts per cage. Sporozoite numbers were detected by dissecting and grinding salivary glands in Schneider's Insect Medium (Sigma) on days 14–18 post feed.

Phenotypic analysis of *Pf abcc2*⁻ parasites in FRG-huHep mice

Pf NF54 *and Pf abcc2*⁻ sporozoites were isolated from salivary glands of infected *Anopheles stephensi* mosquitoes. For analysis of *Pf abcc2*⁻ liver stage, 1×10^6 *Pf* NF54 and 1×10^6 *Pf abcc2*⁻ sporozoites were injected intravenously (retro-orbital) into three FRG NOD huhep mice per group. Livers were harvested on days 2, 3 and 6 and used for IFA. To evaluate for blood stage transition of *Pf abcc2*⁻ in FRG huhep mice, 1×10^5 *PfNF54* and *Pf abcc2*⁻ sporozoites were injected intravenously into two FRG huHep mice per group. On day 6, 400 μL of 70% RBCs were injected intravenously and on day 7, 50μL of blood from each mouse was sent for qPCR analysis to detect parasite 18S RNA. On day 7, two mice per group were euthanized, blood was collected by cardiac puncture, washed three times in asexual media, a volume of human RBCs equal to the packed RBC volume was added and cultured *in vitro*. Fresh media was replaced daily, and cultures were analyzed every 2–3 days by thick smear for presence of parasites for upto 6 weeks. Samples for 18S rRNA qRT-PCR were analyzed every 5–7 days.

To evaluate for blood stage transition of *Pf abcc2*⁻ in FRG NOD huhep mice, 1×10^6 *Pf abcc2*⁻ sporozoites were injected intravenously into 5 FRG NOD huHep mice. On day 6, 400μL of 70% RBCs were injected intravenously and on day 7 and 8, 50μL of blood from each mouse was analyzed by qRT-PCR analysis to detect parasite 18s RNA. On day 8, all mice were euthanized, blood was collected by cardiac puncture, washed three times and transferred to *in vitro* culture as described above. Fresh media was replaced daily, and cultures were analyzed every 2–3 days by thick smear for presence of parasites for upto 6 weeks. Samples for 18S rRNA qRT-PCR were analyzed every 5–7 days.

Plasmodium 18S rRNA qRT-PCR quantification of parasite load

For quantification of *Plasmodium* 18S rRNA from mouse blood, 50 μL of whole blood was added to 2 mL of NucliSENS lysis buffer (bioMérieux, Marcy-l'Étoile, France) and frozen immediately at −80°C.

One mL of lysate was subsequently processed using the Abbott m2000sp using mSample RNA preparation kit (Abbott, Niles, IL). The eluate was tested by qRT-PCR for the pan-*Plasmodium* 18S rRNA target. The qRT-PCR reaction was performed using 35 μL SensiFAST™ Probe Lo-ROX One-Step Kit (Bioline, Taunton, MA) and 15 μL of extracted eluate. Plasmodium 18S rRNA primers/probes (LCG BioSearch Technologies, Novato, CA) were as follows: Forward primer PanDDT1043F19 (0.2 μM): 5′-AAAGTTAAGG GAGTGAAGA-3′; Reverse primer PanDDT1197R22 (0.2 μM): 5′-AAGACTTTGATTTCTCATAAGG-3′; Probe (0.1 μM): 5′-[CAL Fluor Orange 560]- ACCGTCGTAATCTTAACCATAAACTA[T(Black Hole Quencher-1)] GCCGACTAG-3′[Spacer C3]). Cycling conditions were RT (10 min) at 48°C, denaturation (2 min) at 95°C and 45 PCR cycles of 95°C (5 s) and 50°C (35 s).

Immunofluorescence assay of liver stage parasites

FRG huHep mice were injected with one million sporozoites of *Pf* NF54, *Pf abcc2*-mCherry or *Pf abcc2⁻* sporozoites. Livers were harvested on different days post infection, fixed in 4% (vol/vol) paraformaldehyde (PFA, Alfa Aesar) in 1X PBS for 18–24 h in a shaker at room temperature, followed by two washes in 1X PBS for 2 h. 50 μm thick sections were made using a Vibratome apparatus (Ted Pella, Redding, CA). For IFA, liver sections were permeabilized in 1X Tris-buffered saline (TBS) containing 3% (vol/vol) H_2O_2 and 0.25% (vol/vol) Triton X-100 for 2 h at room temperature with gentle agitation. Sections were then blocked in 1xTBS containing 5% (vol/vol) dried milk (TBS-M) for at least 1 h and incubated with primary antibody in TBS-M at 4°C overnight with gentle agitation. After three, 10-minute-long washes in 1x TBS, fluorescent secondary antibodies and 4-,6- diamidino-2-phenylindole (DAPI) at 1 mg/mL were added in TBS-M for 2 h at room temperature in a similar manner as above. After three, 5-minute-long washes in 1x TBS, the section was incubated in 0.06% (wt/vol) $KMnO_4$ for 45 s to quench the background fluorescence. Sections were mounted in polylysine-coated slides overlaid with ProLong™ Gold Antifade Mountant (Molecular Probes, CA) and a coverslip. Primary antibodies used included *Pf* CSP clone 2A10 (1:500), *P. yoelii* BiP polyclonal (1:1000), *P. yoelii* ACP (1:500), *P. vivax* mHSP70 (1:1000) and *Pf* MSP-1 clone 12.10 (1:500, European Malaria Reagent Repository), mCherry clone 16D7 (1:500, Thermo Scientific), *Pf* Exp1 rabbit polyclonal sera (1:200, provided by Klaus Lingelbach). Secondary antibodies include donkey anti-mouse 488, donkey anti-mouse 594, donkey anti-mouse 647, donkey anti-rabbit 488, donkey anti-rabbit 594, donkey anti-rabbit 647 and donkey anti-rat 594. All secondary antibodies were used at a dilution of 1:1000.

Immunofluorescence assay of blood stage parasites

Thin blood smears of *Pf ABCC2^mCherry* parasites were fixed in 100% ice-cold methanol processed for 3 min followed by two washes in 1X PBS at room temperature. Slides were marked with blocked in 2% bovine serum albumin (BSA) for 1 h at room temperature, followed by incubation with primary antibody in 2% BSA overnight at 4°C. Slides were washed three times in 1X PBS, 8 min per wash, followed by incubation with secondary antibodies (1:1000) and DAPI (1 mg/mL) in 2% BSA for 1 h. Slides were washed three times in 1X PBS, 8 min per wash and mounted in ProLong™ Gold Antifade Mountant (Molecular Probes, CA) and a coverslip. Primary antibodies used included *Pf* MSP-1 clone 12.10 (1:500, European Malaria Reagent Repository) and α-mCherry clone 16D7 (1:500, Thermo Scientific). Secondary antibodies include donkey anti-mouse 488 and donkey anti-rat 594. All secondary antibodies were used at a dilution of 1:1000.

Immunofluorescence assay of parasite mosquito stages

Mosquito midguts were dissected in Schneider's insect medium (Gibco™) and fixed with 4% (vol/vol) PFA in 1X PBS for 1 h at room temperature in a microcentrifuge tube. Midguts were washed with 1X PBS and then permeabilized and blocked with 1X PBS containing 3% BSA and 0.25% Triton X-100 for 2 h at room temperature. Midguts were washed with 1X PBS, and primary antibody (were diluted in 1X PBS/3% BSA and incubated with the midguts at 4°C overnight with end-over-end rotation. The primary antibody used was α-mCherry clone 16D7 (1:500, Thermo Scientific). Following three washes with 1X PBS, fluorescent secondary antibodies were diluted with 1x PBS plus 3% BSA and incubated with midguts for 2 h with end-over-end rotation at room temperature. Midguts were washed three times with 1X PBS, stained with 4-,6-diamidino-2-phenylindole (DAPI) at 1 mg/mL in 1X PBS for 5 to 10 min at room temperature, and washed once more with 1x PBS. Midguts were mounted on a polylysine-coated microscope slide and overlaid with

ProLong™ Gold Antifade Mountant (Molecular Probes, CA) and a coverslip. Secondary antibodies include donkey anti-mouse 488 and donkey anti-rat 594.

Salivary gland sporozoites (3 μL) were spotted onto a polylysine-coated microscope slide glass slide (with 12 wells) and allowed to dry overnight. Sporozoites were fixed in 4% PFA for 20 min, followed by 3 washes in 1X PBS. Blocking and permeabilization were carried out together in 2% BSA with 0.02% Triton X-100 for 2 h. Wells were incubated with primary antibody diluted in 2% BSA in PBS overnight at 4°C. Wells were washed three times with 1X PBS, followed by incubation with secondary antibody in 2% BSA in PBS and DAPI for 2 h. Wells were washed three times, a drop of ProLong™ Gold Antifade Mountant was added on each well and a coverslip was carefully placed on the slide. Primary antibodies used included *Pf* CSP clone 2A10 (1:500) and mCherry clone 16D7 (1:500, Thermo Scientific). Secondary antibodies include donkey anti-mouse 488 and donkey anti-rat 594.

Microscopy

All images were acquired using the Stellaris 8 confocal microscope (Leica Microsystems) with 63x water objective and processed using the Lightning software (Leica Microsystems). For quantification of parasite liver stage size, IFA using the CSP antibody was used to measure the area of liver stage parasites. The parasite was assumed to be elliptical in shape and therefore area was calculated from its longest (a) and shortest (b) circumferential diameter (πab).

QUANTIFICATION AND STATISTICAL ANALYSIS

Quantification was represented by the mean ± standard deviation. Calculations and statistical tests indicated in the figure legends were performed using GraphPad Prism Software. The statistical tests used are one-way and two-way ANOVA and unpaired t-test, as indicated. *$p < 0.05$, **$p < 0.01$, ***$p < 0.001$. A p value > 0.05 was considered not significant.